INVESTIGATION OF CARBON FIBER AND FREE-STANDING CARBON NANOTUBE ARRAY ELECTRODES FOR LITHIUM-AIR BATTERIES

by
Matthew Stephens Gonzalez

A thesis submitted to Johns Hopkins University in conformity with the requirements for the degree of Master of Science

Baltimore, Maryland

May, 2016

Abstract: Conventional Lithium-ion battery technology is beginning to approach its practical energy density limit. As the demand for high capacity electrical energy storage increases, the need for a viable replacement to Li-ion batteries is becoming essential. Lithium-oxygen and lithium-air batteries boast a theoretically energy density of 11,140 Wh/kg (compared to gasoline: ~12,330 Wh/kg). However there are many challenges that plague Li-O_2 and Li-air batteries that prevent them from being commercially practical with current technologies. Finding a suitable electrolyte, improving the poor stability of the Li anode, and implementing materials to catalyze the oxygen evolution reaction (OER) and oxygen reduction reaction (ORR) at the air cathode are a few examples of challenges with the technology. Here we report developing a novel method to assemble and test lithium-air batteries constructed from standard Li-ion coin cells using a free standing, pure carbon nanotube array as the porous air breathing electrode, ionic liquid as a hydrophobic electrolyte and lithium foil as the anode. We achieved a Li-air battery capable of remaining stable up to 35 cycles to a depth of 500 mAh/g_{CNTs} over a one week with current densities as high as 250 mA/g while breathing ambient atmosphere. By sputter coating a layer of gold onto our carbon nanotube array air cathodes we achieved a 25% increase in discharge potential when compared to pure carbon nanotubes cathodes. We found that although the addition of gold slightly increased the internal resistance (R_{int}) of the battery it reduced the surface and charge-transfer resistance ($R_{s\text{-}ct}$) by more than 30%. Lithium anode stability still remains a major challenge that plagues our ability to test long life improvements to the air cathode. Investigation of lithium titanate (LTO) as a lithium host remained stable after 50-100

cycles, however a negative discharge voltage arises when assembled as a lithium-oxygen cell. We suspect this may arise from an undercapacity of Li available from the LTO, requiring further testing with higher material loading. We also developed a method to test our batteries under a controlled atmosphere using a pressure vessel. This will in theory mitigate the issue of anode stability, allowing us the ability to test the long-life performance of gold and other catalysts during charge and discharge of a Li-air battery in future studies.

Acknowledgements

For anyone reading this, I am glad you are interested in my work explored energy storage technologies. This work would not have been possible without the support of my friends, colleagues, family and the wonderful professors and staff in both Johns Hopkins Materials Science and Engineering and Chemical and Biomolecular Engineering departments. Firstly I would like to thank my family for support and most importantly paying for my education here. They encouraged me during my 5 years at JHU to do the best I could. I would also like to thank my friends and lab-mates in Dr. Chao Wang's group. David Raciti taught me the workings of the lab during my years of research with the group. Without him, I don't think any of this would have been possible. Dr. Lei Wang and Jerome Fineman where my two partners in crime in our battery research group. I want to thank my other friends in the group for making my research experience so enjoyable. I also want to thank Dr. Chao Wang for mentoring me and providing the space and funding to explore nanotechnology during my multiple years working under him.

I want to thank Dr. Orla Wilson for being a huge support and always willing to have a chat…I still need to take her up on that offer for a beer. I want to thank the various facilities and staff at JHU, particularly Dr. Michael McCaffery and the JHU IIC, and Bryan Crawford in Materials Science and Engineering characterization.

While my time at Hopkins was wonderful, I am very excited to be moving on and pursuing a PhD at the University of California San Diego in Nanoengineering.

Table of Contents:

List of Figures:

I. An Introduction

A. Energy Storage Status Quo

Humans consume more than 14 TWh of energy per year and is projected to triple by the year 2050. Currently over 80% of the world's energy is produced from fossil fuels with petroleum products generating the largest fraction, followed by coal and natural gas[1]. However, burning these fossil fuels has caused a marked increase in the level of atmosphere greenhouse gasses, spurring climate change and increased global temperatures. Anthropogenic carbon dioxide is one of the main contributors to greenhouse gasses and is produced largely from the burning of fossil fuels. The amount of CO_2 present in our atmosphere is only projected to increase as mankind continues to power itself with fossil fuels **[Figure 1]**[2,3].

Despite the low cost and current surplus of oil, with a barrel of oil currently costing under $50[4], many countries have agreed to place sanctions on greenhouse emissions with the goal to mitigate and reverse much of the damage from unregulated fuel consumption and to conserve the remaining finite fuel reserves. This has led to a huge increase in the demand to develop new clean and renewable energy sources. Solar, wind, tidal and hydrothermal are a few of the more explored alternatives to fossil fuels, however the energy is often generated during non-peak hours and storing it remains a huge challenge. Therefore, in order for these renewable energy sources to be a viable

replacement for our current fossil fuel based infrastructure, large-capacity grid energy storage devices must be developed. While the market for grid storage is in its infancy and was worth only $200 million dollars in 2012, it has been growing dramatically and is expected to a $20 billion dollar industry by next year[5].

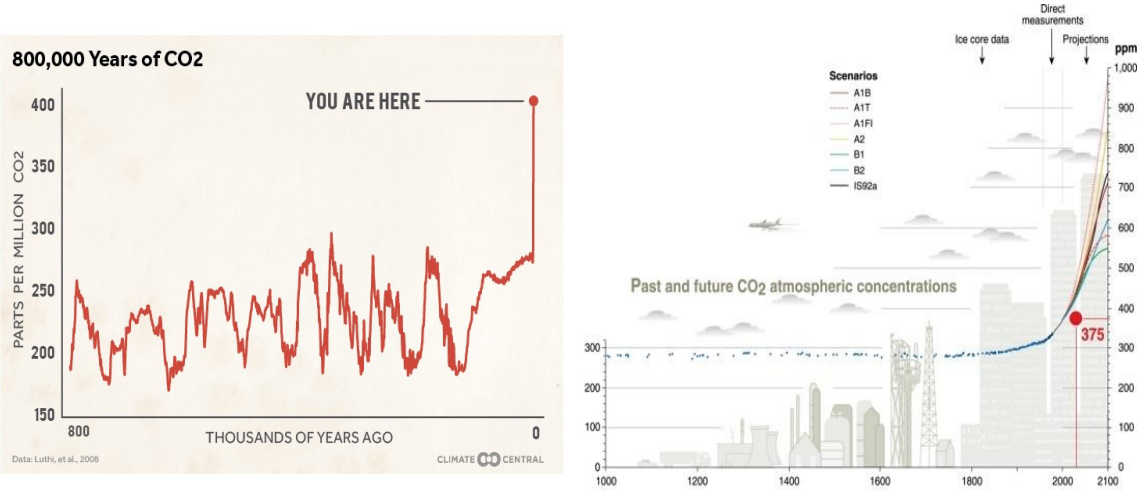

Figure 1: **a)** Measurement of the CO_2 levels in the Earth's atmosphere from the past 800,000 years. Notice the sharp vertical peak of CO_2 in the past century. **b)** A graph from the U.S. Department of Energy showing past and projected atmospheric CO_2 concentrations. This data was taken in 2008 and since then CO_2 reached a 400 ppm milestone. CO_2 levels have increased nearly 25% since NASA began gathering data in 1958 and is project to continue increasing at an alarm rate.

**Figures adapted from U.S. Department of Energy*

The need for high capacity energy storage is not limited to grid storage with interest extending into electric transportation. The auto industry has also begun making efforts to transition away from fossil fuel based vehicles, however, the limited range and high price of electric cars remain barriers preventing main stream adoption of the technology **[Figure 2]**[6]. Current lithium-ion batteries systems can only achieve a range of about 100 miles on a full charge. Modern commercial lithium-ion batteries have achieved specific energy densities of up to 160 Wh/kg, with next generation silicone anode Li-ion promising to narrow the gap between the maximum theoretical energy density of ~400 Wh/kg[7]. Even at the theoretical limit Li-ion cannot contend with the energy density of gasoline, requiring a completely new breed of batteries to meet our ever growing demands

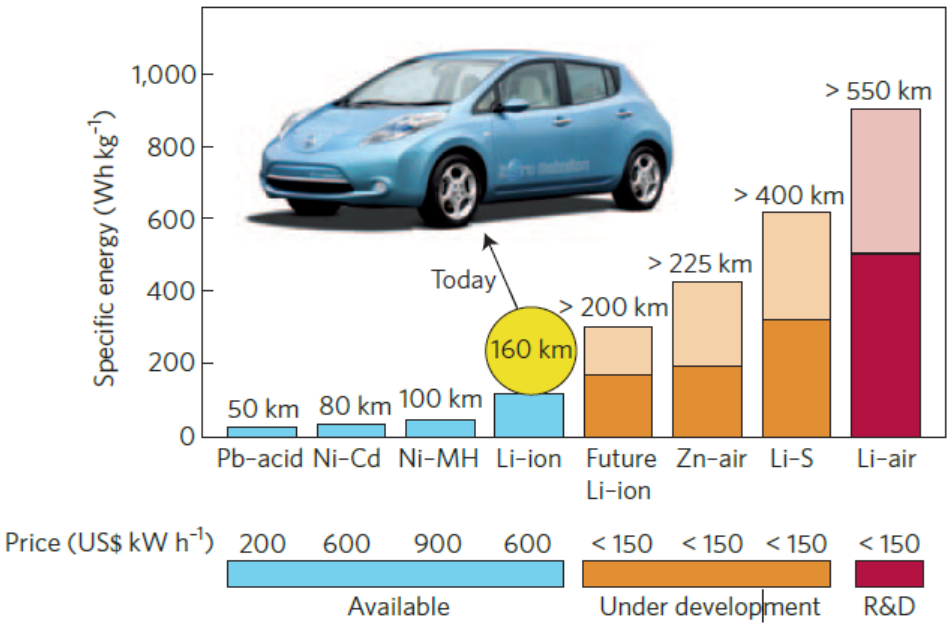

Figure 2: Comparison of specific energy density (Wh/kg) of various battery chemistries as well as price per kWh.

Figure adapted from Nat Mater **11, 19–29 (2012)*

B. Discovery of the Lithium-Oxygen Battery

The lithium-oxygen battery chemistry was first discovered at Lockheed in the 70's but was abandoned due to lithium's high reactivity with the aqueous electrolytes available at the time[8]. With the introduction of organic electrolytes the first rechargeable Lithium-oxygen battery was introduced in the 90's by *Abraham et al.*[9] Lithium-oxygen batteries offer a possible solution to the need for high-capacity energy storage devices boasting a specific energy density of 11,140 Wh/kg. When compared to the specific energy density of gasoline, roughly 13,000 Wh/kg, it is easy to see how Li-O_2 may become a viable technology to store large amounts of energy [**Figure 3**][10]. This large energy density arises from the unique chemistry of Li-O_2 battery. The Li-O_2 system can be compared in some aspects to a fuel cell, and is often considered a lithium battery-fuel cell hybrid[11]. This similarity to a fuel cell allows for "free" oxygen to enter and exit the battery without the need to count the weight of oxygen when calculating specific energy

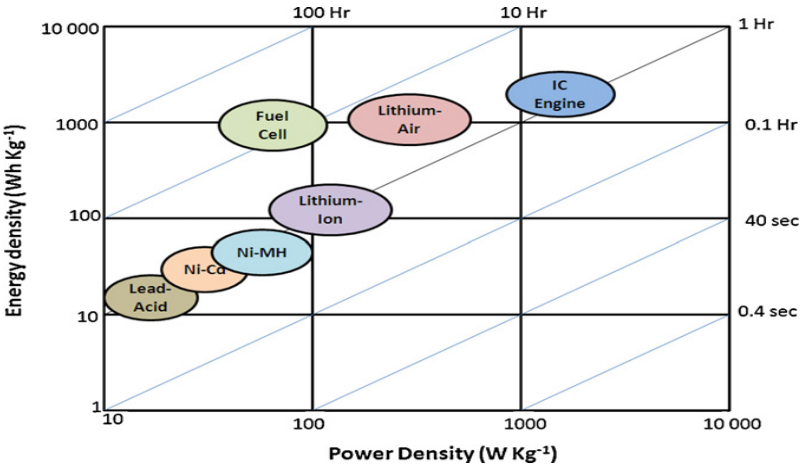

Figure 3. Ragone plot comparing energy densities and power densities of various energy storage systems. **Figure adapted from Journal of Power Sources **196,** 4436–4444 (2011).*

density[12]. It should also be noted that oxygen is not included in the calculations for the specific energy density of gasoline.

II. Challenges of Lithium-Oxygen and Lithium-Air Batteries

A. Reaction Pathway Selectively and Product Deposition Control

With the unique chemistry of the lithium-oxygen battery come many benefits as well as challenges. Selectively controlling the products as Li reacts with O_2 is one aspect that greatly influences the stability of the battery. Since the battery requires oxygen to freely enter and exit the cell, a porous air cathode is required to "breathe" oxygen while remaining stable throughout extended use **[Figure 4]**[13]. This selectively is effected by a number of factors including the electrolyte environment and the kinetics of the reaction which can be altered through catalysts[10]. The anode also presents a significant challenge in developing a stable system. Lithium metal is highly reactive and very sensitive to the presence of moisture. Li is also notorious for forming dendrites that can puncture the separator membrane causing battery failure[14,15]. The many challenges facing the Li-O_2 and Li-air battery give rise to a difficult problem with no one simple solution and requires precise control of every aspect of the battery.

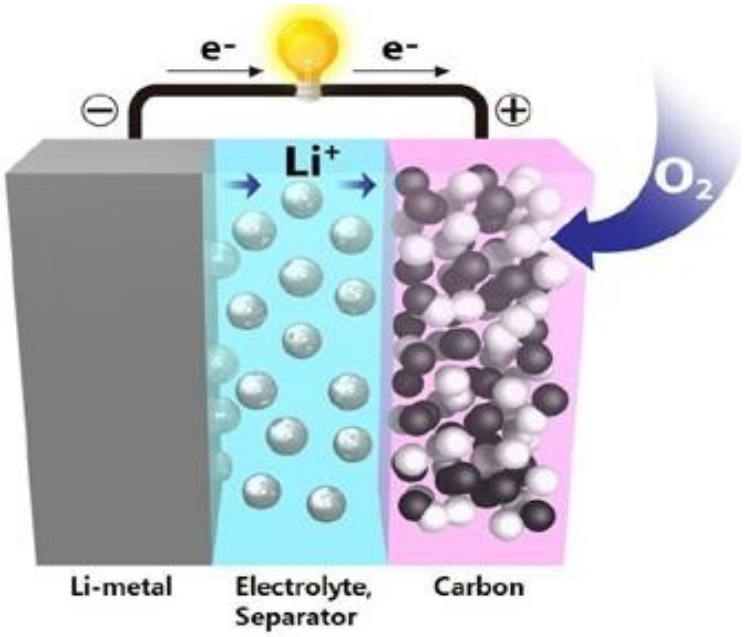

Figure 4: Schematic of a discharging lithium-air battery. O_2 flows into the porous carbon based cathode and reacts with Li^+. O_2 is liberated and Li^+ forms lithium metal at the anode during charge. *Figure adapted from Nature Chemistry **4**, 579–585 (2012)*

The suspected reaction pathways taken at both the anode and cathode are poorly understood and variant on a verity of factors, most prominently the electrolyte environment. During discharge lithium metal is oxidized to ionic form at the anode yielding electrons in the discharge step and reduced back to metallic form during charge **(1)** described as followed:

$$Li \leftrightarrow Li^+ + e^- \quad (1)$$

The reduction of oxygen can occur through a reversible two-electron pathway **(2)** or through a non-reversible four-electron pathway **(3)** and the overall reactions can be simply expressed as[16]**:**

$$2Li + O_2 + 2e^- \leftrightarrow Li_2O_2 \ (E° = 2.91 \text{ V vs. } Li/Li^+) \quad (2)$$

$$4Li + O_2 + 4e^- \rightarrow 2Li_2O \quad (E° = 2.96 \text{ V vs. } Li/Li^+) \quad (3)$$

Each half cell potentials are the standard potential associated with the respective reaction and can be verified with the Nernst Equation **(4)**:

$$\Delta E = \Delta E° - \frac{RT}{nF} \ln Q \quad (4)$$

However it is not as simple as these three reactions; there are a many proposed electrochemical reactions occurring at the cathode involving multistep electron-transfer processes and various oxygen species including O^{2-}, OH^-, O_2, HO^{2-}. One mechanism proposed by *Laoire et al.*[17] that has garnered much attention involves the formation of an intermediate lithium superoxide in a one electron process **(5)** which further reacts with an additional electron and lithium ion to form Li_2O_2 **(6)** described as followed:

$$O_2 + e^- + Li^+ \rightarrow LiO_2* \quad (3.0 \text{ V vs } Li/Li^+ \quad (5)$$

$$LiO_2* + e^- + Li^+ \rightarrow Li_2O_2 \ (3.0 \text{ V vs } Li/Li^+) \quad (6)$$

It has also been suggested that Li_2O_2 will be further discharged forming Li_2O, severely limiting the cyclability of the system[18]. Even with complete selectivity towards the reversible Li_2O_2 product it is still very important to physically control product deposition to maintain porosity. These many unknowns and potential reactions make it difficult to understand and control the electrochemistry and kinetics of Li-O_2 systems.

B. Low Roundtrip Efficiency

While having a higher specific energy density, Li-O_2 batteries have a lower working potential (~2.5-3.0 V vs Li/Li^+) than a conventional high power Li-ion batteries (~3.7 V vs Li/Li^+) **[Figure 5]**[19,20]. The low round trip efficiency the Li-air system is also a major issue, making it necessary to decrease the voltage gap between charging and discharging. The sluggish kinetics of the ORR during discharge and OER during charging give rise to this low efficiency, but it has been found that the introduction of catalysts can greatly improve the charge and discharge voltages[21]. Recent studies show that gold nanoparticles can greatly improve the discharge voltage, platinum nanoparticles can greatly improve the charge voltage, and Au/Pt alloy nanoparticles can act as a bifunctional catalyst to improve the overall roundtrip efficiency dramatically[22]. Due to the high cost of these precious metals, alternative catalysts have also been explored.

Manganese dioxide has been shown to be a viable bifunctional catalyst as well, improving the performance of the air breathing cathode[23].

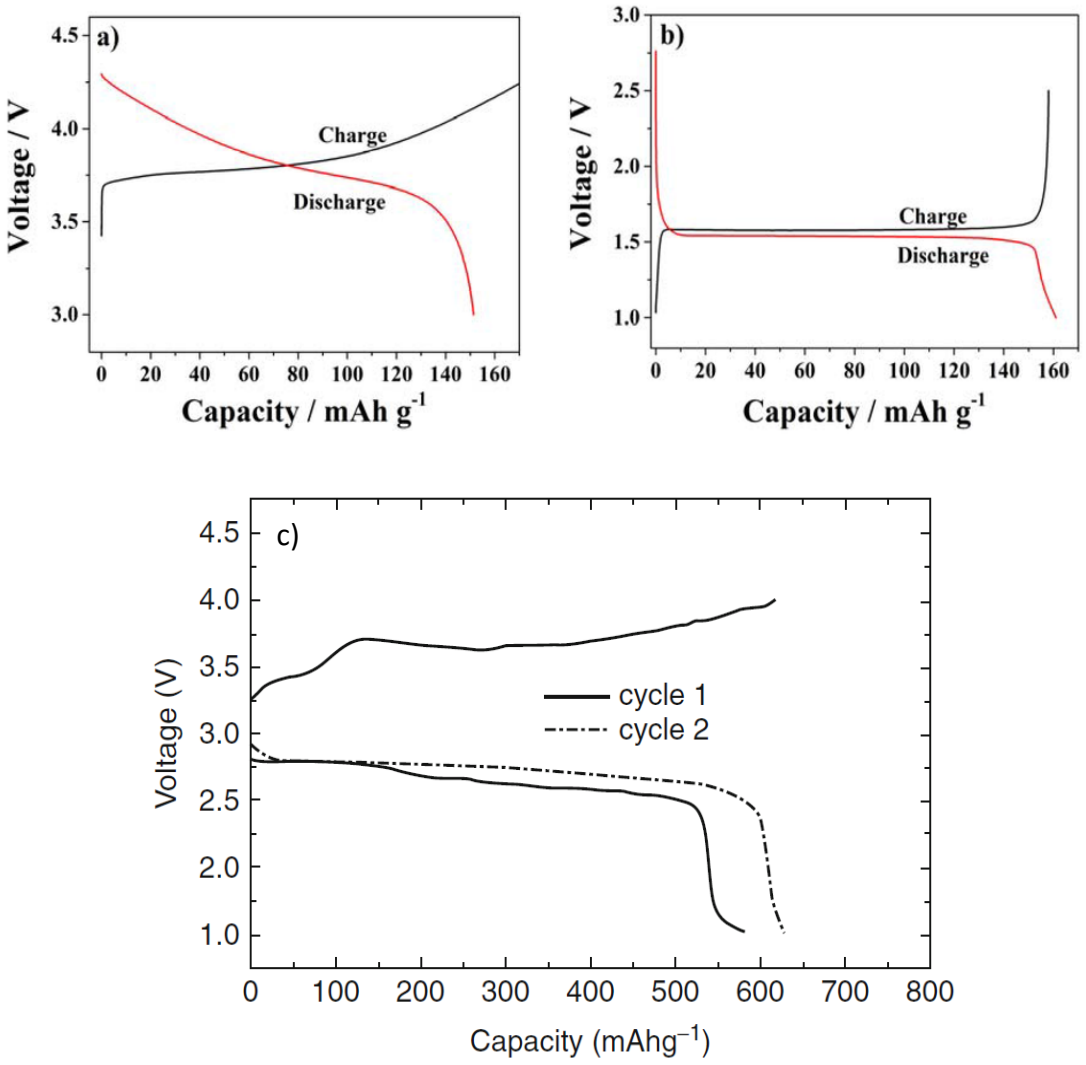

Figure 5: Typical lithium-ion battery charge/discharge plots of **a)** NMC (LiNiMnCo) battery and **b)** lithium titanate (Li_2TiO_3). **c)** Typical lithium-oxygen battery charge/discharge plot.

Figures adapted from J. Electrochem. Soc. 143, 1–5 (1996) and Membranes 5, 632–645 (2015)

C. Porous Air Electrode

One of the main challenges preventing full realization of a secondary (rechargeable) Li-O_2 battery is allowing O_2 to reversibly enter and exit the system. In order for the battery to "breathe" in air, the cell must be constructed with an air porous electrode. Since the Li_2O_2 and Li_2O are formed in this porous electrode, the buildup these products can clog the pores preventing further oxygen from entering or exiting the system, severely limiting the capacity and cyclability of the battery. Work has been done to physically control the deposition of discharge products to maintain porosity by introducing dummy nucleation sites[24] as well as implementing novel, albeit complex architectures such as columns and nanoarrays[25]. The ideal air electrode must have the following requirements: 1) High electronic and ionic conductivity 2) Allow for and maintain fast oxygen diffusion over the life time of the battery 3) stability in the electrolyte environment during operation and 4) effective catalysts to improve OER and ORR kinetics and selectivity.

D. Environment Control

In theory the same chemistry occurs in a lithium-oxygen cell and in a lithium-air cell, however this is far from true. Generally testing of these battery system is performed in a pure O_2 environment. Earth's atmospheric composition obviously has many more

constituents besides O_2 **[Figure 6]**, most critical to the performance of the battery being carbon dioxide and moisture which can enter the cell and result in undesirable and irreversible side reactions. It is well known that lithium metal is highly reactive to moisture reacting to form LiOH and H_2, rendering traditional aqueous electrolytes useless. Carbon dioxide is highly soluble in the organic solvents often used in Li-O_2 batteries and will form Li_2CO_3 and both then anode and cathode[26]. Therefore it is essential to control the gasses that enter the cell and ideally isolate it to pure O_2 while in natural atmosphere.

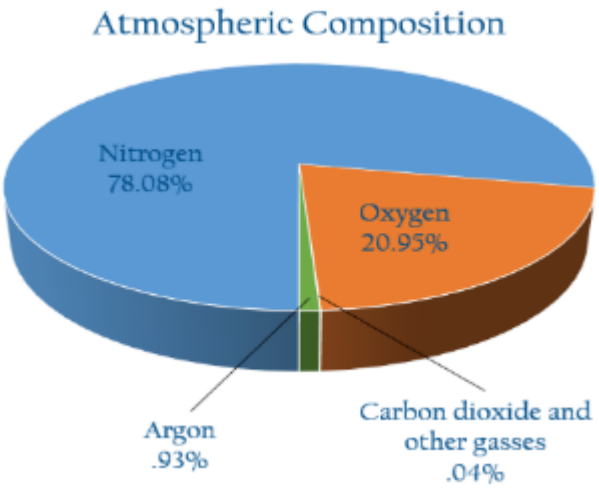

Figure 6: Earth's atmospheric composition comprised of mainly nitrogen and oxygen with trace amounts of carbon dioxide and other gases.

E. Suitable Electrolytes and Separator Membranes

One route being explored for open air electrolytes that has gained interest is using ionic liquids. With stability towards lithium metal, a large working voltage window and high ionic conductivity, ionic liquids offer a promising alternative to organic electrolytes. Due to their low vapor pressure at room temperature, ionic liquids would allow for long term use without fear of drying out and causing battery failure. Also ionic liquids are known to be hydrophobic, aiding in the prevention of moisture penetration. In terms of overall safety, ionic liquids are often non-volatile and non-flammable, a huge consideration in battery construction[27]. However challenges with the ion conducting membrane arises when using ionic liquid electrolytes including wettability and stability. The trilayer polypropylene-polyethylene-polypropylene membrane most commonly used in Li-ion batteries are not wetted due to the hydrophobicity of ionic liquids preventing Li^+ migration from anode to cathode. The membrane must also remain stable within the ionic liquid while at the working potentials of the battery throughout its lifetime and maintain a barrier between electrodes to prevent shorting.

F. A Complete System

In order to develop a reliable lithium-air system a high level of control over every aspect of the battery is required, demanding clever engineering and outside-of-the-box thinking. By optimizing and troubleshooting piece by piece, it should be possible to develop a battery that can vastly out-perform current energy storage technologies. While the challenges may be great, the benefits that lithium-air batteries offer could revolutionize mankind's energy infrastructure.

III. Oxygen Evolution and Reduction Reaction Catalysts

Initially we focused our investigation on the role that nano-scale catalysts play in the oxygen evolution and reduction reactions that occur at the air cathode. Gold is known to be a highly active ORR catalysts and has been shown to greatly increase the working voltage during discharge[15]. Using organic solvent methods it possible to synthesis a wide range of highly controllable nanoparticles with various morphologies and compositions. The main focuses of our studies were catalytic improvements on charge and discharge potential, cyclability, Li_2O_2 selectivity and deposition control.

A. Gold Nanoparticles

i. Synthesis:

We began with the synthesis of gold nanospheres. While there are myriad methods to synthesize gold nanoparticles, we needed an easily tunable and scalable method. By modifying a method developed by Hiramatsu & Osterloh[28] we were able to synthesize highly monodisperse gold nanoparticles. Size and morphology was determined with transmission electron microscopy **[Figure 7 a]**. The TEM model information can be found in section **1.a** of the supplementary information. Toluene is used to control reaction temperature while oleylamine (OAM) is used as the surfactant and reducing

agent. The method to synthesize highly monodispersed ~20 nm gold nanoparticles is as follows:

1.5 mL of OAM (70% laboratory grade, purchased from Sigma Aldrich) and 25 mL of toluene was brought to reflux in a three neck flask with a schlenk line setup under constant stirring. The system was purged with N_2 gas while heating to reflux, at which the outlet was closed to prevent the toluene from evaporating off and kept under a N_2 blanket. Gold(III) chloride hydrate, $HAuCl_4$, (99.999%, purchased from Sigma Aldrich) was dissolved in 0.6 mL of OAM and 0.5 mL of toluene. This was then injected into the flask and the final solution was kept at reflux for 2 hours. A color change from clear/yellow to a deep red occured. After cooling to room temperature, the solution was mixed in a 1:1 ratio with EtOH and centrifuged at 8000 RPM for 10 minutes to precipitate out the gold nanoparticles from solution. The nanoparticle were then redispersed in either hexanes, chloroform or toluene.

By controlling the concentration of gold chloride various sizes can be synthesis. Further synthetic methods are described in section **5.a** and **5.b** of the supplementary information.

ii. Gold-Carbon Electrostatics and Adhesion

Our next step was to deposit these gold nanoparticles onto a porous air electrode. It was possible to deposit these gold nanoparticles directly on carbon fiber paper solely through electrostatic attraction. We tested a number of dispersants to determine which would create the most uniform deposition and determined that chloroform achieve the most uniform dispersion. Scanning electron microscopy was used to examine the nanoparticles on carbon fiber paper **[Figure 7.b]**. The model of the SEM can be found in section **1.b** of the supplementary information. The method to attach the nanoparticles onto the carbon paper is very simple and results in reproducible control over the loading of gold.

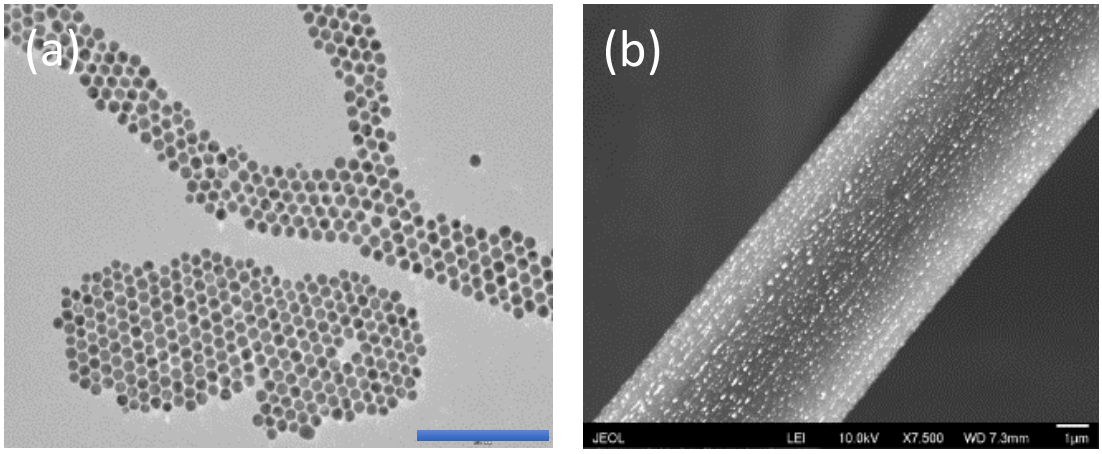

Figure 7. (a) Transmission electron microscopy of ~20 nm gold nanoparticles, scale bar represents 200 nm. (b) Scanning electron microscopy using lower secondary electron image detector (LEI) of gold nanoparticles electrostatically attached to carbon fiber paper by ultrasonication in chloroform dispersed NPs.

Synthesis Method:

Nanoparticle that were dispersed in solution after synthesis were precipitated out by adding dispersed NPs to 200 proof ethanol in a 1:1 ratio and centrifuged at 8000 RPM for 10 minutes. This causes the nanoparticles to accumulate on the side of the centrifuge vial, allowing the liquid to be poured off. They were redispersed again in chloroform and this processes is repeated up to two more times to remove excess surfactant. The nanoparticles are centrifuged for a final time and dried overnight. After being weighed they can be redispersed chloroform to a concentration of choosing.

Carbon paper is cut into 17 mm disks and sonicated in ethanol to remove any dust and other contamination. A single carbon paper disk is then placed into a scintillation vial with the chloroform dispersed nanoparticles. Reproducible loading of 0.2 mg of NPs was achieved with 2.5 mg of Au NPs was dispersed in 1 mL of chloroform and sonicated for 1 hour.

The results of the dispersion hexanes and toluene can be found in supplementary information section **2.a**. In order to remove the surfactants remaining on the surface of the nanoparticles that would potential hinder electrochemical activity, the loaded carbon paper was annealed at 185° C overnight. An SEM study shows that very little aggregation had occurred during the annealing process **[Figure 8]**. This sample was loaded with approximately 1 mg of Au to examine aggregation at a higher loading. This was done by dispersing 25 mg of NPs in chloroform and using our sonication method.

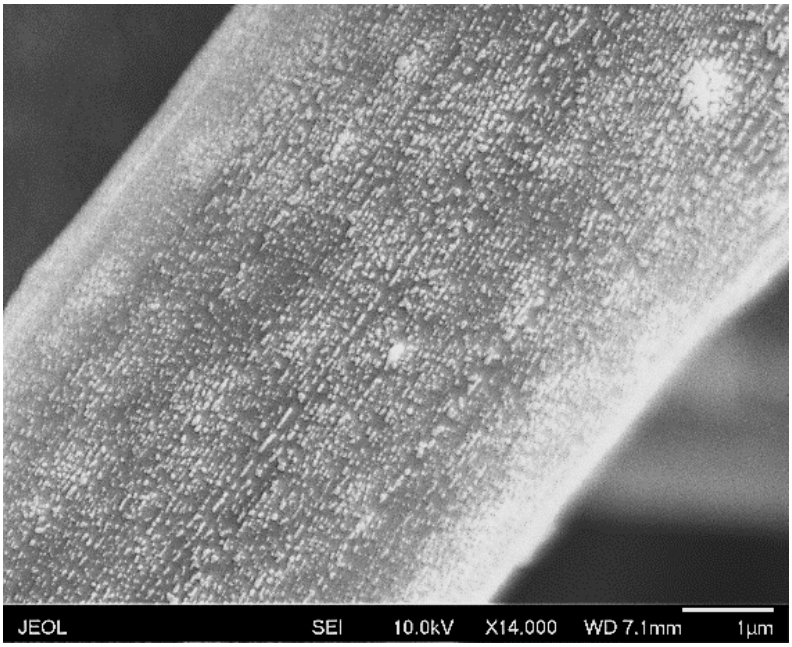

Figure 8: SEM using secondary electron image detector (SEI) of~20 nm gold nanoparticles attached to carbon paper using the ultrasonication method after being anneal at 185° C overnight. Slight aggregation has occur, but the major of the NPs remain unaggregated.

B. Gold Nanowires

We also were interested in examining the performance of different morphologies of Au catalysts in Li-O_2 batteries. Our next study focused on the synthesis and incorporation of Au nanowires into our battery system to improve OER during discharge.

i. Synthesis & Deposition

The nanowire synthesis was based on simple method developed by Kang and Murray[29] using CO as a reducing agent and oleylamine as the surfactant. This methods allows for the synthesis of very long and thin, hair-like Au nanowires **[Figure 9 a]**. The synthesis process is as followed:

An initial solution of 0.046 g of AuCl (99.9% trace metal basis, purchased from Sigma Aldrich) in 20 mL of chloroform and 1.84 mL oleylamine was made in a three neck flask. This solution was under constant stirring at 600 RPM while being heated under N_2. Chloroform acts as a temperature control, reaching reflex at roughly 60° C. As soon as the solution reached reflux, the N_2 flow was switched off and replaced with CO. The CO was introduced into the flask at a rate of 15 cm^3/min. Reduction of AuCl by CO was allowed to occur for 10 minutes before the CO inlet was closed and N_2 was reintroduced while the solution was brought to room temperature. A color change from clear/yellow to red/brown was noticed as nanowires formed. The solution was mixed in a 1:1 ratio with EtOH and centrifuged at 8000 RPM for 10 minutes to precipitate out the nanowires from solution. The nanowires were then redispersed in either hexanes, chloroform or toluene.

The nanowires were also deposited onto carbon fiber paper. However, unlike the gold nanoparticles, the nanowires were deposited using a drop casting method **[Figure 9 b]**. The sonication method resulted in a loss of wire morphology during deposition, which is

shown in supplementary information section **2.c**. However one potential downside of this method is that Au nanowires may not be able to deposit as deeply and uniformly into the bulk of the carbon fiber paper when compared to the sonication method.

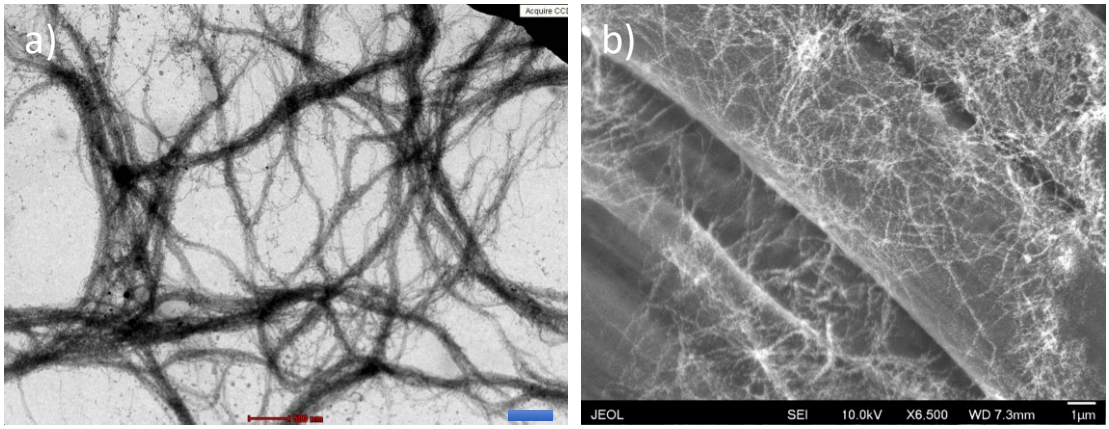

Figure 9: a) Transmission electron micrograph of Au nanowires, scale bar represents 500 nm. b) Scanning electron micrograph of Au nanowires drop casted onto carbon fiber paper.

ii. Thermal Instability

Similar to the synthesis of Au nanoparticles, the nanowire synthesis also used oleylamine as a surfactant to mediate crystal growth. Because of this the Au nanowires required annealing to remove surfactants that would hinder electrochemical activity as well. The nanowires underwent the same annealing treatment as the nanoparticles. Unlike the nanoparticles, the wires were not stable up to 185° C **[Figure 10 a]**. The wires

broke apart into the individual segments. We also attempted to remove the surfactants using an acetic acid wash which only requires temperatures of 40° C. However, that too resulted in the decomposition of the nanowires **[Figure 10 b]**. Interestingly enough though, the nanoparticle segments that formed remained to dot where the nanowire had been deposited.

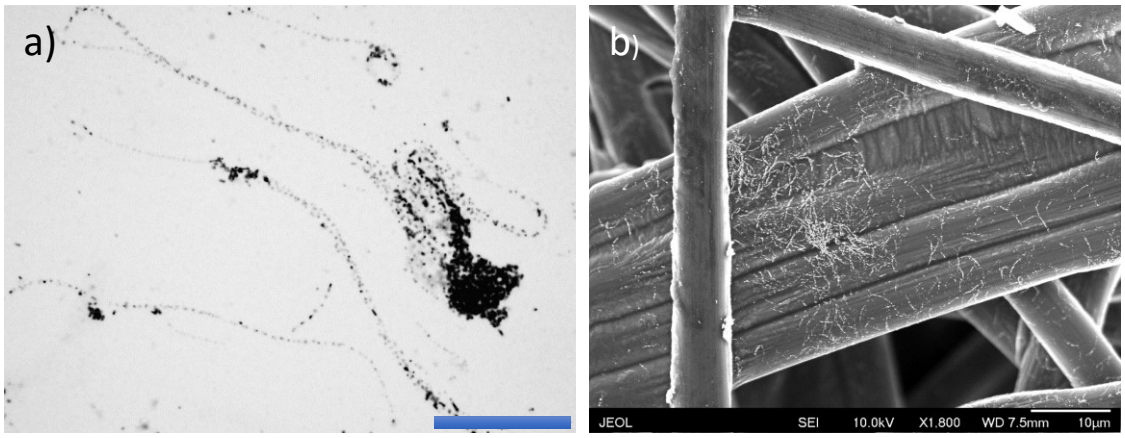

Figure 10: a) TEM of decomposed Au nanowires annealed at 185° C overnight on copper TEM grid showing thermal instability of these wires, scale bar represents 1 µm. b) SEM of Au nanowires washed using acetic acid at 40° C overnight on carbon fiber paper.

C. Oxygen Cell Charge/Discharge Testing

i. Carbon Fiber Paper

During the process of developing novel carbon fiber paper-gold cathodes we measured their performance in pure O_2 to establish a benchmark using galvanostatic charge/discharge test performed on an Arbin BT 2000 linear battery testing system. We measured both charge and discharge potentials as well as the capacity of our batteries among other things. These tests have many limits and parameters that can be set to yield a broad view or pinpoint analysis of battery performance. The main parameters we modified were current density, voltage limits and capacity limits. The parameters of each test are listed in the caption of each figure.

The batteries tested were assembled in a MTI lithium battery air cell **[Figure 11].** The components were stored and assembled in a glovebox with the H_2O and O_2 levels below 0.5 ppm. The carbon paper—with and without Au—was used as the air electrode. Glass fiber paper was used as the separator. 1 M Lithium perchlorate ($LiCl_4$) dissolved in dimethylsulfoxide (DMSO) was the electrolyte. Lithium metal, separator, and carbon paper were stacked in the cell respectively and wetted with .3 mL of electrolyte. The cell was then flushed and pressurized with pure O_2 to 15 psi above atmospheric pressure to develop a benchmark performance before begin tests in ambient atmosphere.

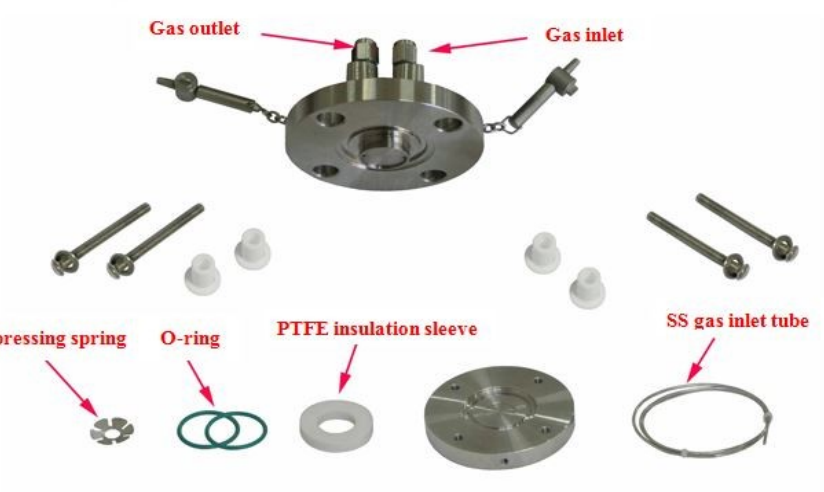

Figure 11: MTI EQ-STC-LI-AIR split test lithium-oxygen cell.

We first measured the performance of carbon paper without the addition of any Au as a control to compare performance and improvement against **[Figure 12 a]**. The initial discharge capacity achieved on the first cycle was over 400 mAh/$g_{carbon\ paper}$, but quickly

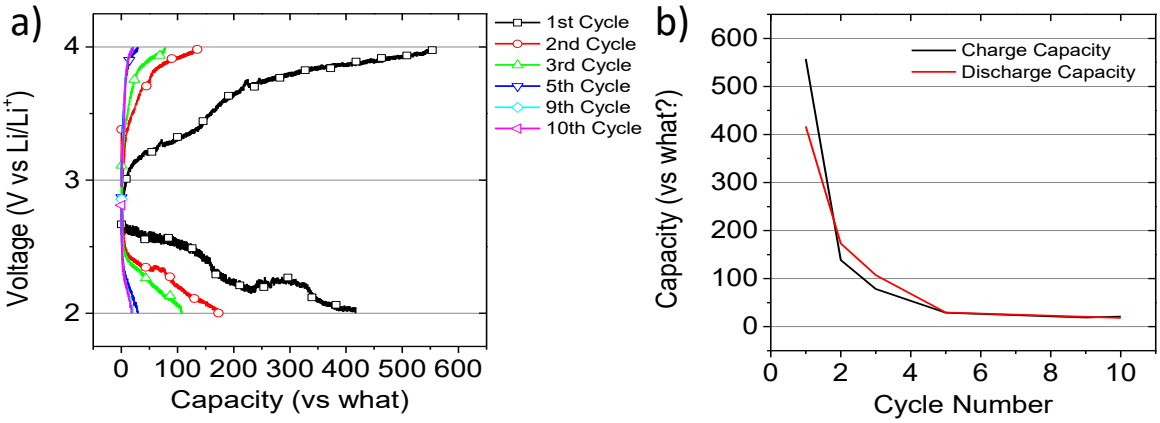

Figure 12: a) Voltage vs Capacity plot for the first 10 cycles of plain carbon fiber paper cathode. **b)** Capacity vs cycle number for first 10 cycles of this cathode. The current density was 50 mA/g, the voltage was limited from 2.0 - 4.0 V, and there was no capacity limit.

fell off. By the second cycle the discharge capacity had halved, and by the tenth cycle discharge capacity was nearly non-existent **[Figure 12 b]**. *Ex Situ* SEM analysis after failure reveals a coating of discharge products which is most likely the ultimate cause of failure **[Figure 13]**.

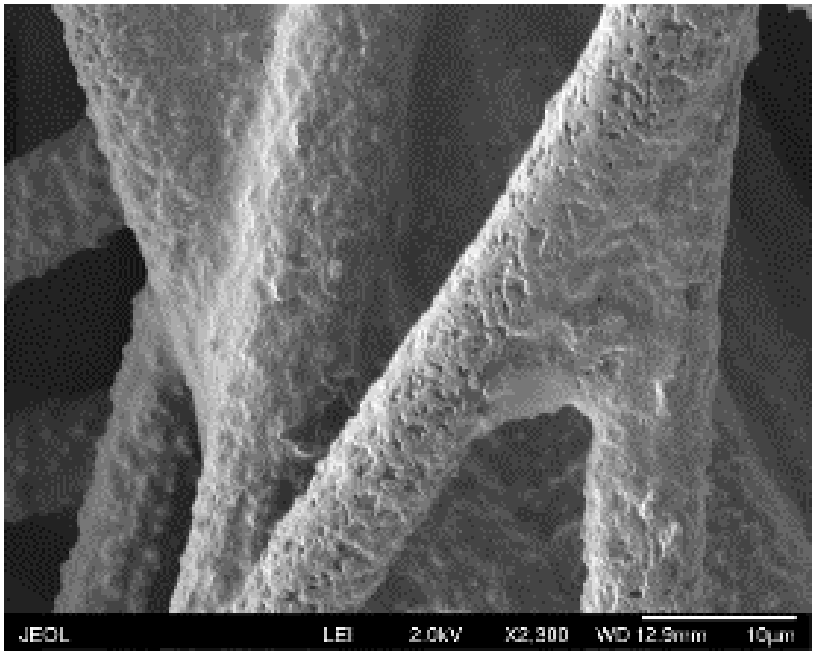

Figure 13: Carbon fiber paper cathode removed after 10 cycles, ending on charge. The carbon fiber is almost completely covered in irreversible discharge product causing capacity fade and ultimately battery failure.

ii. Addition of Gold:

We then tested carbon fiber paper that had been sonicated in the ~15 nm Au nanoparticle dispersion using the method previously described. There was marked improvement in the performance of the cathode, with the initial two discharge capacities achieving double over the plain carbon paper. The discharge voltage was much more stable as well **[Figure 14 a]**. Cyclability was poor however, and the battery again failed by the 10th cycle **[Figure 14 b]**. Au nanoparticles detached from the carbon fiber paper during cycling and discharge product failed to fully convert back into Li and O_2 during charging. Backscatter SEM reveals a uniform coating of nanoparticles underneath the first discharge product, but by the 10th cycle all but a few nanoparticles remain **[Figure 15]**.

We also noticed that the charge capacity was dramatically less than discharge. This most likely impacted cyclability and could be aided by an OER catalysts such as Pt or Pd.

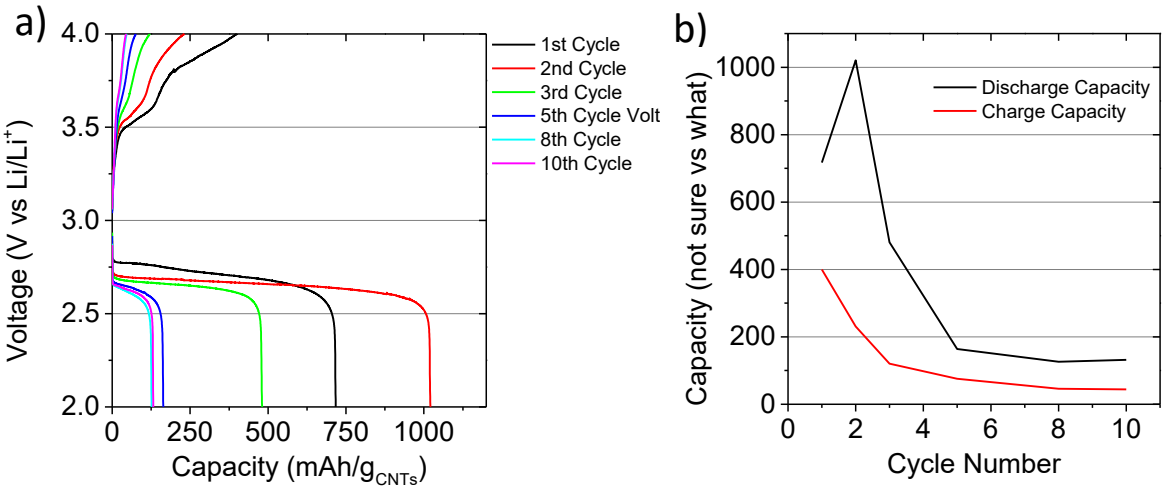

Figure 14: a) Charge-discharge and **b)** cycle capacity plot for Au nanoparticle coated carbon fiber paper.

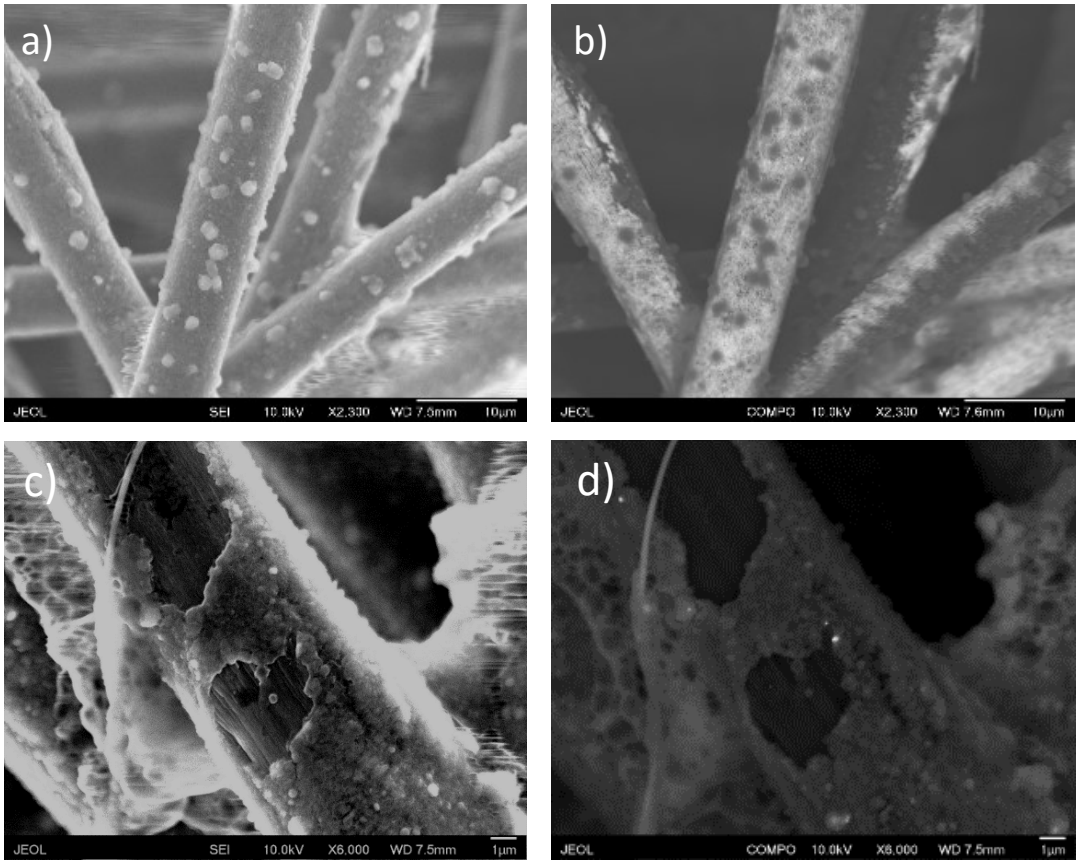

Figure 15: Scanning electron micrograph of carbon fiber paper with gold nanoparticles after a single discharge using **a)** secondary electron imaging showing a layer along with clusters of discharge product and **b)** backscatter electron imagine showing gold nanoparticles underneath the discharge product. Carbon fiber paper after 10 cycles stopped after charge using **a)** secondary electron imaging and **b)** backscattered electron imaging showing almost no remaining gold nanoparticles.

IV. Free-Standing, Pure Carbon Nanotube Arrays Cathode

Since it appeared the carbon fiber paper would not be a sufficient cathode to introduce and study various nanoparticle, we developed a free-standing air cathode using arrays of single wall carbon nanotube (SWCNTs or CNTs) **[Figure 16]**. SWCNTs are known for their high electrical conductivity and for being one of the strongest materials known to exist. By depositing a water dispersion of CNTs we were able to develop a binder free, interlaced array directly on glass fiber filter separators which were directly used in the battery. The binder free nature of this electrode coupled with glass fiber's ability to absorb large amounts of electrolyte allows for thorough wetting throughout the array. This created the critical three-phase boundary between electrolyte, electrode and oxygen at which the electrochemical reactions can occur. CNTs have been found to maintain good electrochemical performance in an ionic liquid environment as well[30], critical for our system. Facile integration of a wide range of catalysts into the array is possible without dramatic various to the method we developed.

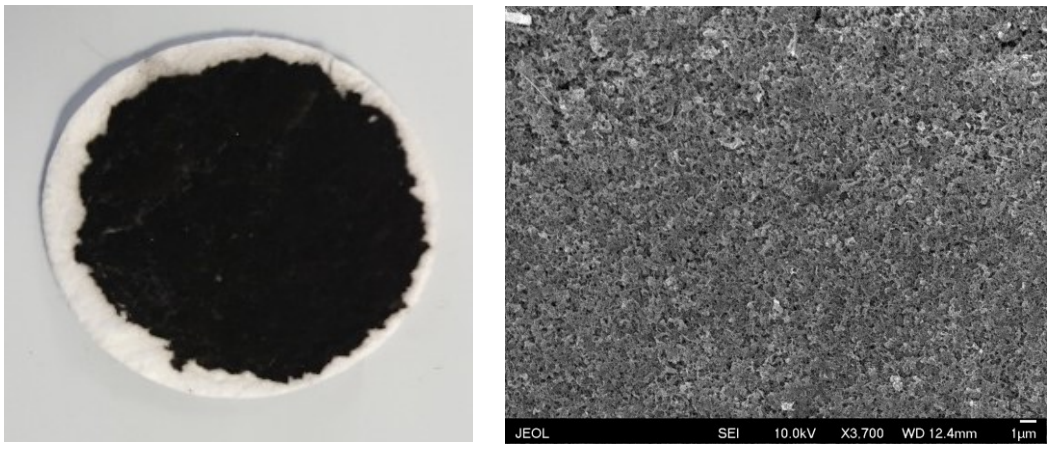

Figure 16: a) Carbon nanotubes deposited on glass fiber paper using vacuuming filtration. **b)** Scanning electron micrograph of CNTs array on glass fiber.

Deposition Method:

A commercial 1wt% water dispersion of single wall carbon nanotubes was purchased from US Research Nanomaterials. The SWCNTs had an average length of 5-30 µm and an outer diameter of 1-2 nm. This dispersion was treated with a water soluble surfactant that allow the normally hydrophobic CNTs to disperse in water. The stock solution was diluted in deionized water to a concentration of .05 mg/mL and ultrasonicated for 10 minutes to guarantee uniform dispersion. Advantec Grade GF75 glass fiber filter membranes with a pore size 0.3 µm were purchased from Cole-Parmer and punched to a diameter of 19 mm. These were ultrasonically washed in ethanol three times to remove any dust and contaminates. A clean glass fiber membrane was placed on a standard vacuum filter where a mask of aluminum foil was place over top. A 15 mm diameter hole was punched into the center of the foil to control the area of deposition.

The top reservoir of the vacuum filter was filled with the diluted nanotube dispersion and allowed to filter through. Since the length of the CNTs is longer than the pore size of the filter, an array of nanotubes was left behind on the filter paper roughly the size of the hole in the aluminum foil. The CNT/glass fiber was rinsed with deionized water to disperse and remove residual surfactant from the CNT surface. The electrodes were allowed to dry in a vacuum oven overnight at 70° C before use.

To create fully free standing electrode **[Figure 17],** 50 mg of CNTs was dispersed onto a PVDF filter membrane and allowed to dry overnight at 70° C in a vacuum oven wherein the CNT array delaminated from the membrane surface. SEM of was performed to examine the array structure and confirm porosity. Interestingly we determined that the CNTs tend to gather into bundles since the thickness of the observed end bundles was greater than the 1-2 nm diameter of the individual CNTs. The structure still maintained a porous, interlace of these bundles however.

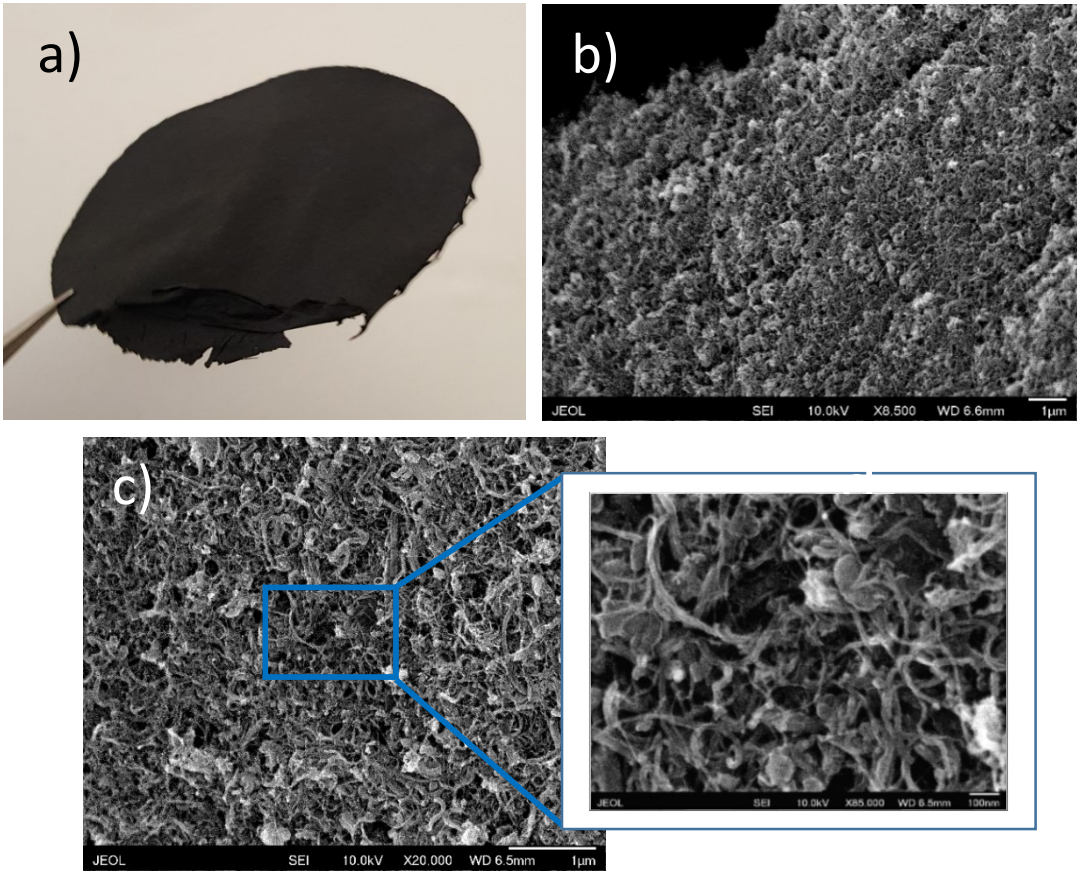

Figure 17: a) Digital photograph of a freestanding CNT array. Scanning electron micrograph of **b)** edge of the CNT array under 8,500x magnification, **c)** top surface of the array under 20,000x magnification, **d)** top surface of the array under 85,000x magnification.

V. Ionic Liquid Electrolytes

Aqueous electrolytes were ruled out as a suitable almost immediately after the discovery of Li-O_2 due to Li metal's reactivity to H_2O. Carbonate-based liquid electrolytes are also known to form Li_2CO_3 when interacting with carbon based electrodes. This led us to studying ionic liquids as the electrolyte in our system. Ionic liquids are essentially liquid salts at room temperature. They are unique in that no solvent is required to form a liquid phase electrolyte. In developing a system to function in ambient atmosphere, we invested ionic liquid electrolytes due to their low volatility, stable voltage window and hydrophobic properties.

EMIM-TFSI (1-ethyl-3-methylimidazolium bis(trifluoromethylsulfonyl)amide) has been shown to be a suitable electrolyte for systems similar to ours[31]. Lithium-TFSI salt (purchased from Sigma Aldrich) was dissolved in EMIM-TSFI (purchased Millipour) in a ratio to yield a 1 M concentration of lithium ions in solution. This was allowed to stir overnight to insure the Li-TFSI salt fully dissolved. The solution was then anneal in a dry, argon atmosphere at 80° C for 24 hours and increased to 120° C for 48 hours to fully dry the electrolyte.

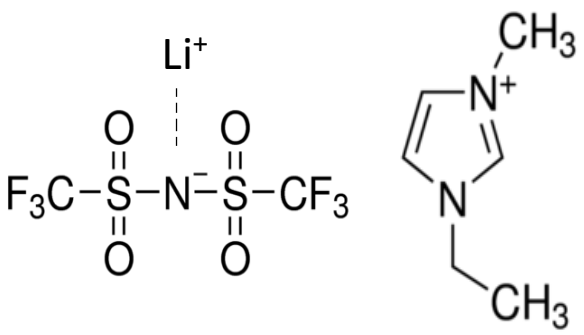

Figure 18: Structure of EMIM-TFSI ionic liquid/lithium salt.

VI. Air Breathing Coin-Cells

For this study we developed a system that allowed us to test Li-air batteries with a simple and inexpensive modification to standard Li-ion battery coin cell casings. The CR2032 coin cells shells along with stainless wave springs and spacer disks were purchased from MTI. A 12 mm hole was punched into the positive casing to allow for air to flow into and out of the system.

Coin Cell Assemble:

The assembly of the coin cells was performed in an argon filled glove box where the O_2 and H_2O levels were maintained below 0.5 ppm. First a stainless steel spacer disk was placed into a negative shell to fill void space and improve contact within the battery. A 19 mm disk, 50 mg, of Li foil (99.99% purchased from MTI) was place on top of the spacer inside of the negative shell. It is important to polish the surface of the Li foil to exposed active, unoxidized Li surface. The foil was completely covered with a 0.1 mL layer of ionic liquid. Next a glass fiber separator was place over the lithium foil and wetted further with 0.1 mL of ionic liquid. As mentioned before, the conventional trilayer Li-ion separator membrane is not wetted by the ionic liquid and therefore cannot be used in this system. A glass fiber membrane with a CNT array was then placed with the CNTs side facing upwards. This is also wetted with another 0.1 mL of ionic liquid to insure a sufficient amount of electrolyte within the cell. A nickle foam air

permeable current collector was punched out to a diameter of 16 mm and placed directly on the CNTs/glass fiber. The modified positive shell was placed over top and crimped with 500 psi using an MTI hydraulic crimping press.

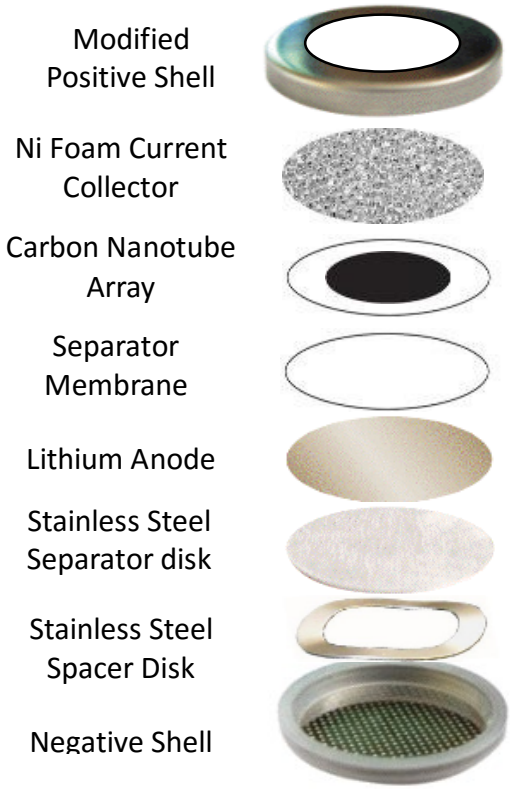

Figure 19: Schematic of our lithium-air coin cell using easily modified conventional Li-ion coin cell casings.

This experiemental design allows us to tests many coin cells similtaniously using the Arbin linear battery tester **[Figure 20]**, increasing the rate we can gather data. Batteries can often take months to fully test—the longer the better—so it is crucial to have the capability to study a large number of batteries in parallel.

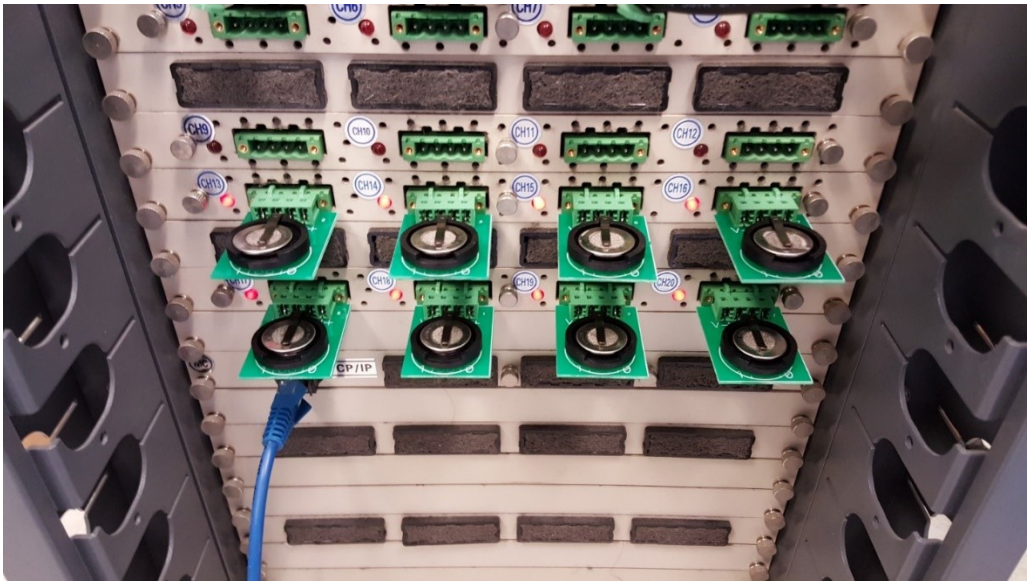

Figure 20: Lithium-air coin cell being studied in Arbin linear battery tester.

VII. Cyclability and Stability Testing

A. Initial Galvanostatic Testing

We were primarily interested in examining the cyclability and overall stability of our Li-air coin cells. We limited capacity artificially to a shallow charge/discharge depth of 1,000 and 500 mAhg/g_{CNT} (commercial Li-ion battery cyclability testing is usually performed at ~120 mAh/$g_{active\ materials}$). The exact parameters of each test are describe in the figure caption.

Initial tests were performed almost immediately after assembly in the glove box. Cycling began in discharge since the Li-air batteries are assembled in a charged state. The battery failed by the 3rd cycle after 5 days in ambient air **[Figure 21]**. We then allowed the battery to rest for 12 hours in a state where no current load is applied both before testing and after every charge. This improved cyclability and resulted in a more stable charge and discharge voltage profile **[Figure 22]**. Likewise, beginning with charging yield similar results without the need to rest 12 hours between cycles **[Figure 23]**. We believe this is because self-discharge products formed during the initial 12 hour rest releases O_2 into the electrolyte during the first charge. The remained of our tests began with charging. We were also able to increase the current density from 50 mAh/g_{CNTs} to 250 mAh/g_{CNTs} and reach 18 cycles before failure **[Figure 24]**. None of our batteries intial remained stable past 5 days, with most failing between 4 and 5 days.

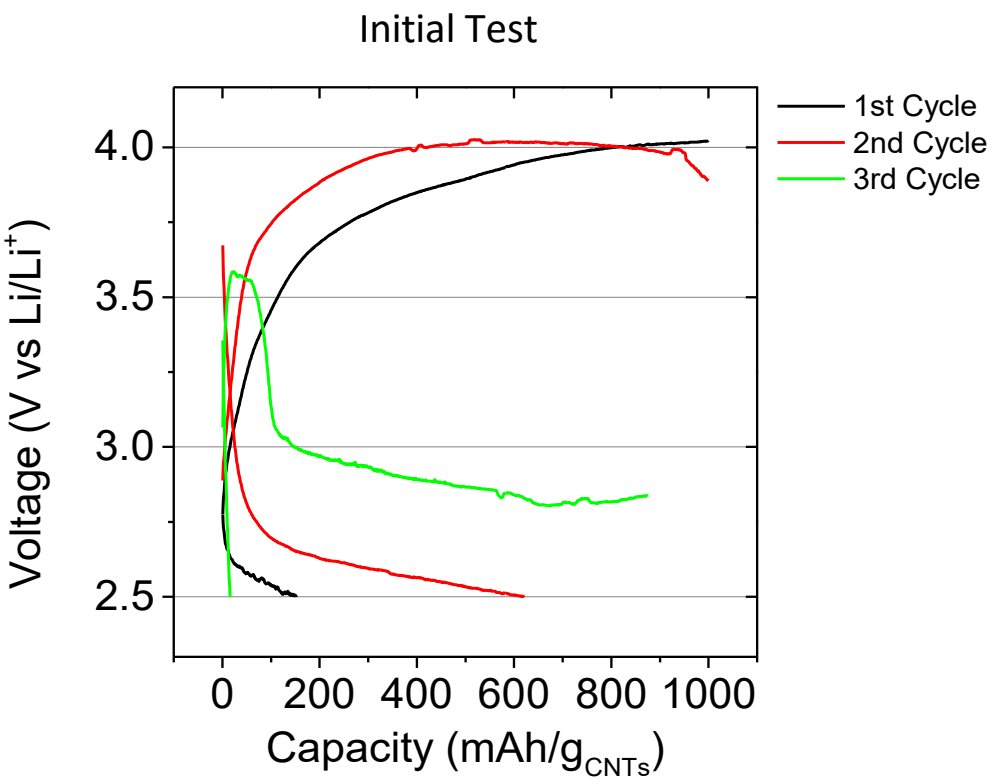

Figure 21: Discharge/charge curve of Li-air coin cell. The battery architecture consisted of a lithium metal anode, 1 mg of CNTs on glass fiber cathode, glass fiber separator membrane, and 0.3 mL of EMIM-TFSI electrolyte. An artificial capacity limit of 1000 mAh/g_{CNTs} was set with a voltage limit set to 4.2-2.5 V. The battery was discharged first and all cycles had a current density of 50 mA/g_{CNTs}. The battery remained stable until the 4th cycle, failing after 5 days.

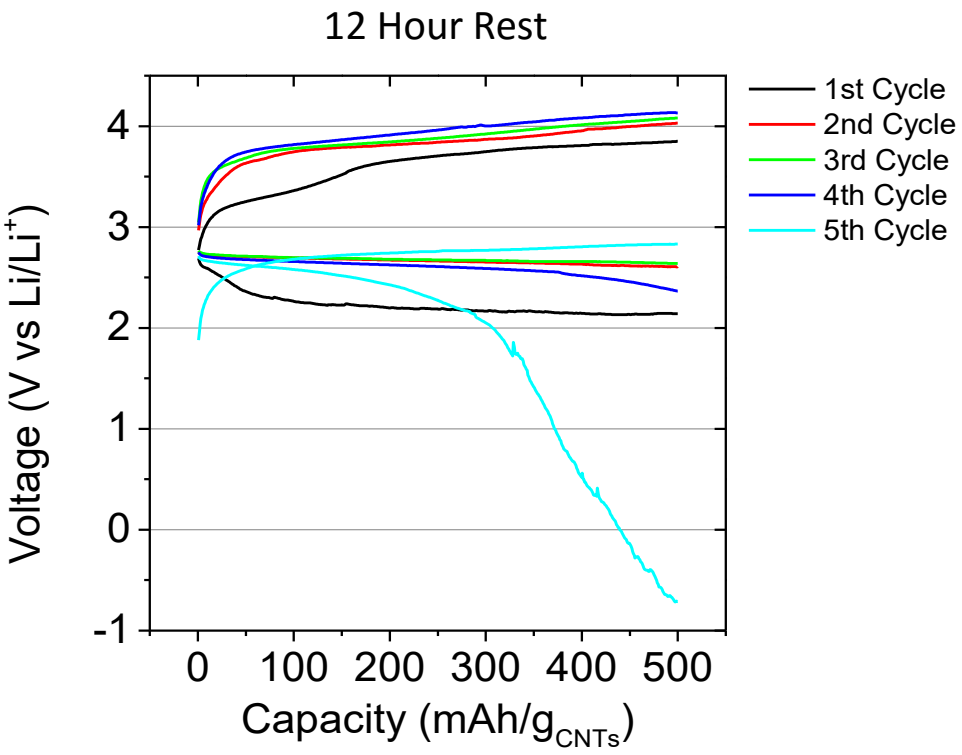

Figure 22: Discharge/charge curve of Li-air coin cell**.** The battery architecture consisted of a lithium metal anode, 1 mg of CNTs on glass fiber cathode, glass fiber separator membrane, and 0.3 mL of EMIM-TFSI electrolyte. An artificial capacity limit of 500 mAh/g_{CNTs} was set with no voltage limit. The battery was discharged first and all cycles had a current density of 50 mA/g_{CNTs}. The battery was allowed to rest with no current load for 12 hours initially and after each charge to allow O_2 diffusion back into the electrolyte. The battery remained stable until the 4^{th} cycle, failing after 5 days.

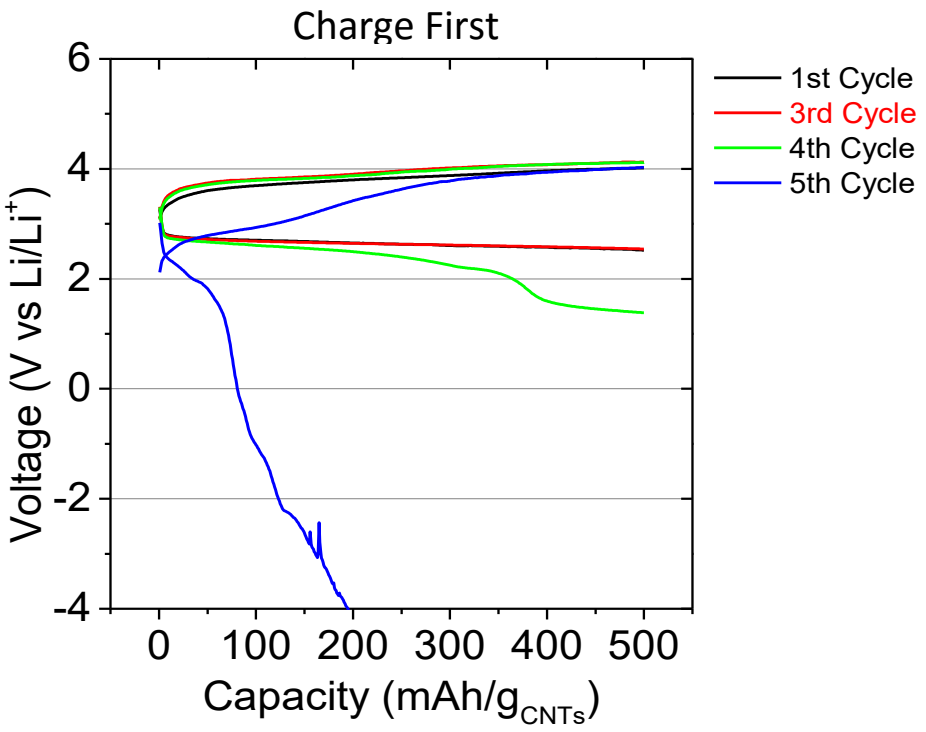

Figure 23: Charge/Discharge curve of Li-air coin cell**.** The battery architecture consisted of a lithium metal anode, 1 mg of CNTs on glass fiber cathode, PVDF separator membrane (0.1 µm pore size), and 0.3 mL of EMIM-TFSI electrolyte. An artificial capacity limit of 500 mAh/g_{CNTs} was set with no voltage limit. All cycles had a current density of 50 mA/g_{CNTs}. The battery remained stable until the 4th cycle, failing after 4 days. *Note: due to an error in the test schedule, the first discharge went back into discharge briefly before it was correctly charged. This did not have an apparent effect on the battery.

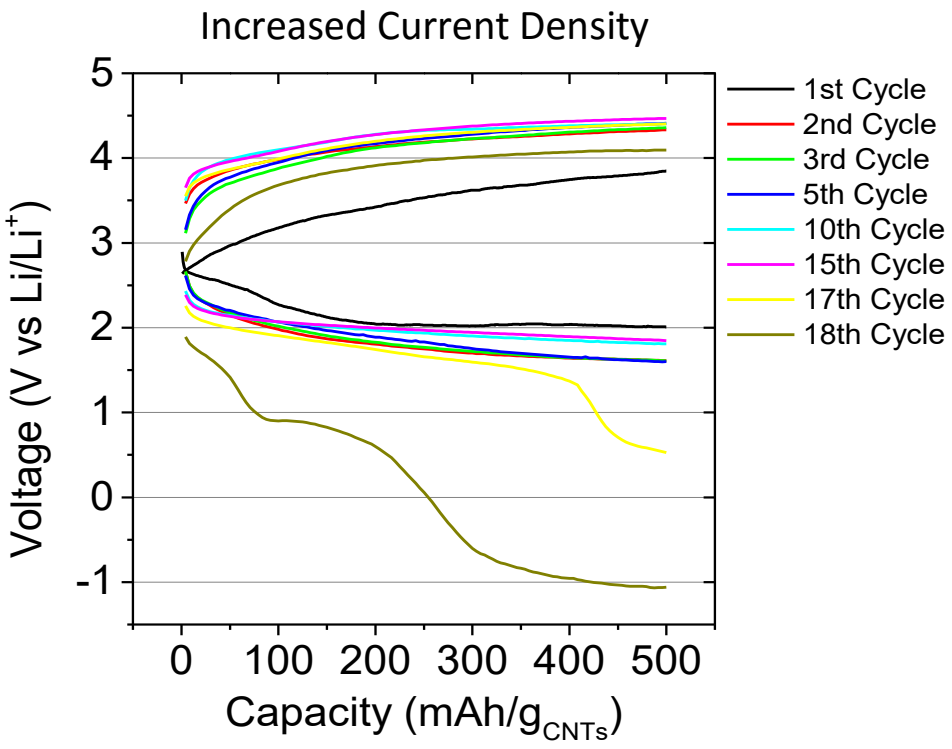

Figure 24: Charge/Discharge curve of Li-air coin cell**.** The battery architecture consisted of a lithium metal anode, 1 mg of CNTs on glass fiber cathode, PVDF separator membrane (0.1 µm pore size), and 0.3 mL of EMIM-TFSI electrolyte. An artificial capacity limit of 500 mAh/g_{CNTs} was set with no voltage limit. The first cycle had a current density of 50 mA/g_{CNTs} and subsequent cycles were set to 250 mA/g_{CNTs}. The battery remained stable until the 17th cycle, failing after 4.5 days.

B. Gold Sputter Coated CNTs Cathodes

Once we had an air breathing Li-O_2 battery stable enough to cycle we returned our attention to the catalytic aspect of the air electrode. We examined the effects that sputter coating layers of Au directly on our CNTs array had on our cathodes. We compared pure CNTs arrays to arrays sputter coated for 30 and 120 seconds at 10 mA **[Figure 25]**. Sputter coating allows for precise metal deposition using argon ions to transport individual Au atoms to the surface of our electrode. While it is difficult to

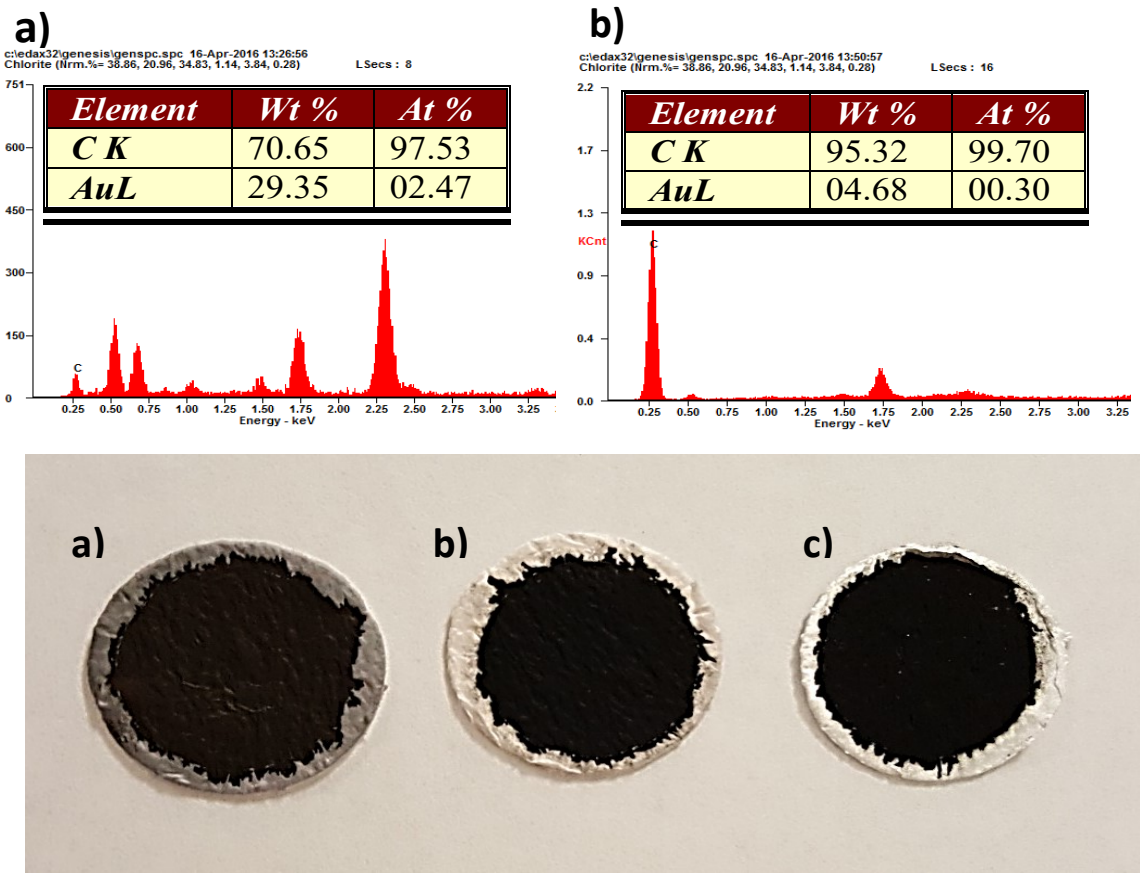

Figure 25: Digital photograph and SEM-EDAX of 1 mg of CNTs Au sputtered at 10 mA for **a)** 120 seconds, **b)** 30 seconds **c)** and pure CNTs.

directly measure the thickness of the deposited layer, we were able to gather a more quantitative measure of the amount of gold using SEM-EDAX. We assembled batteries in the same method as describe before, albeit using sputter coated electrodes.

We repeated testing pure CNTs cathodes to get a standard to compare performance to **[Figure 26]**. Air electrodes that were sputter coated for 30 seconds showed an improvement in the discharge potential of the battery which is as expected since Au is highly active OER catalyst **[Figure 27]**. Air electrodes that were sputter coated for 120 seconds surprisingly seemed to improve the charging potential of the battery **[Figure 28]**. The initial discharge potential for the 30 second sputtered cathode remained above 2.5 V for the entirety of discharge whereas it fell below 2.0 V for both the pure CNTs and 120 second sputtered cathode. During the first charge the 120 second cathode mostly remained below 3.0 V while the 30 second cathode charged above 4.0 V. We also performed impedance tests using an Autolab PGSTAT302N potentiostat/galvanostat from .01-100,000 hz with a 5 mV amplitude on these cells before charge/discharge to measure the internal resistance (R_e), and surface and charge-transfer resistance ($R_{s\text{-}ct}$). We found that the addition of gold slightly increased the internal resistance of the battery but reduced the surface and charge-transfer resistance by more than 30%, which measures the resistance of product—Li_2O_2 and Li_2O—formation **[Figure 29]**. The addition of Au also appeared to increase the life time of the battery by around 50% as a whole. Due to time constraints post failure *ex situ* examination was not performed.

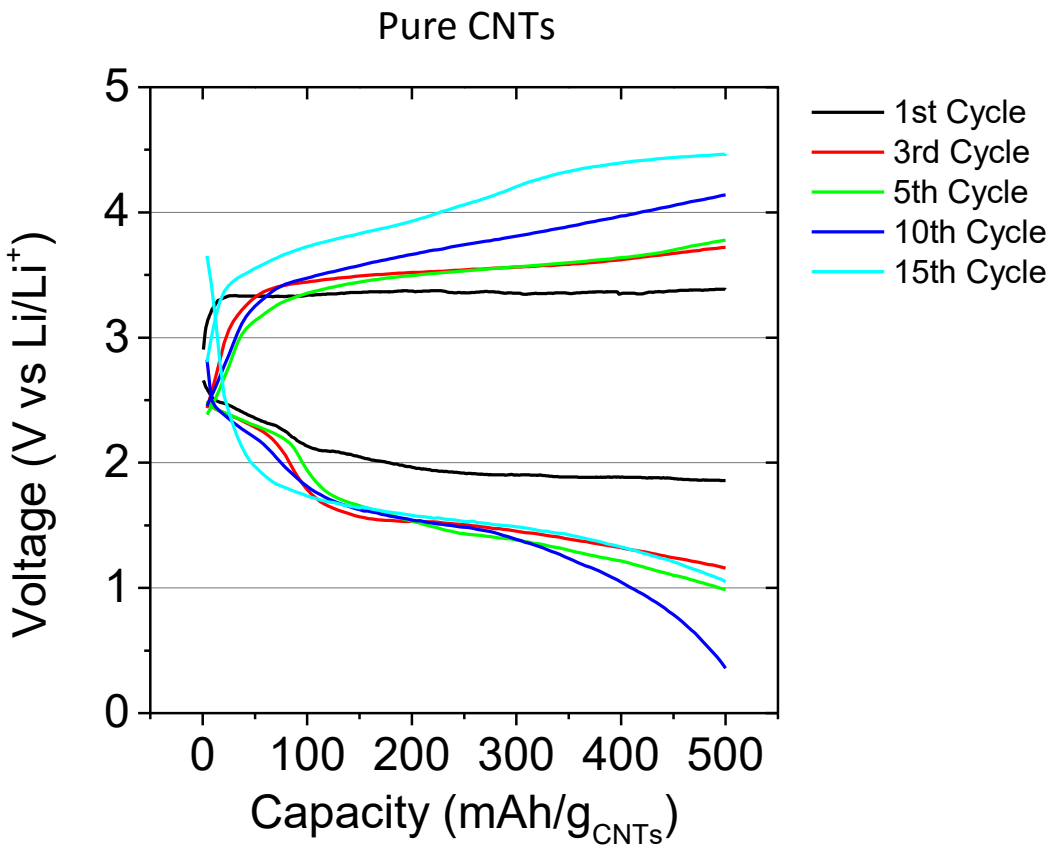

Figure 26: Charge/Discharge curve of Li-air coin cell**.** The battery architecture consisted of a lithium metal anode, 1 mg of CNTs on glass fiber cathode, glass fiber separator membrane, and 0.3 mL of EMIM-TFSI electrolyte. An artificial capacity limit of 500 mAh/g_{CNTs} was set with no voltage limit. The first cycle had a current density of 50 mA/g_{CNTs} and subsequent cycles were set to 250 mA/g_{CNTs}.

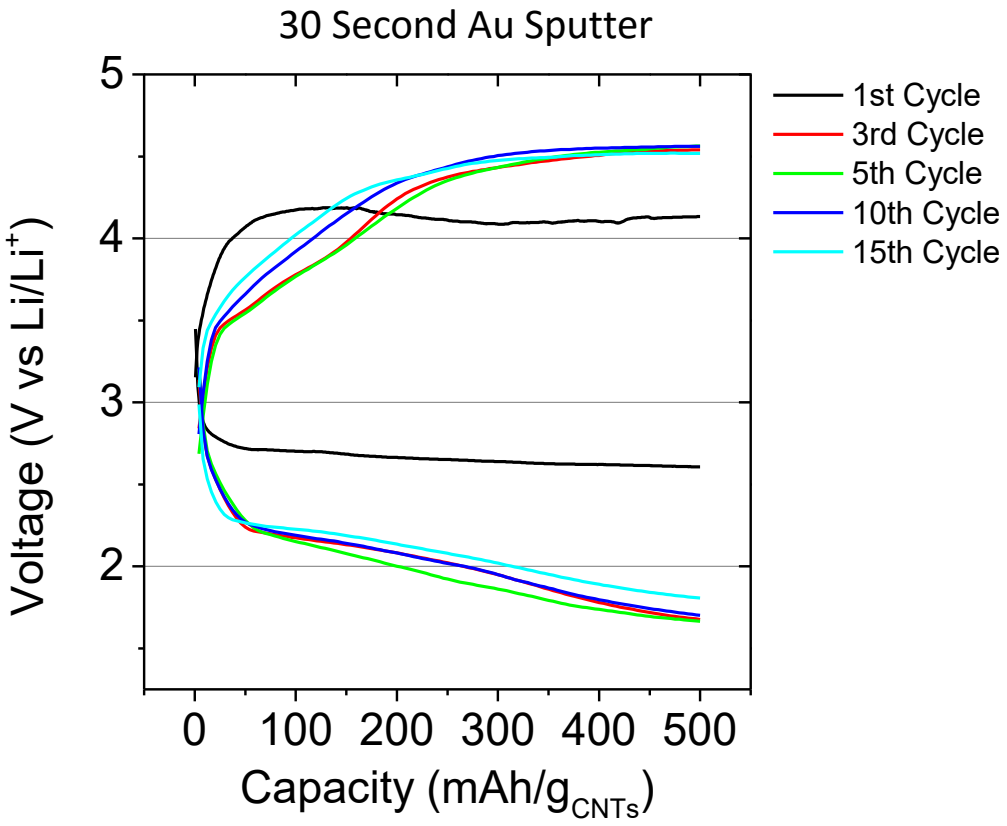

Figure 27: Charge/Discharge curve of Li-air coin cell**.** The battery architecture consisted of a lithium metal anode, 1 mg of CNTs on glass fiber cathode that was sputter coated with Au for 30 seconds, glass fiber separator, and 0.3 mL of EMIM-TFSI electrolyte. An artificial capacity limit of 500 mAh/g_{CNTs} was set with no voltage limit. The first cycle had a current density of 50 mA/g_{CNTs} and subsequent cycles were set to 250 mA/g_{CNTs}. There is a marked improvement in the discharge potential when compared to pure CNTs and 120 second sputtered CNTS.

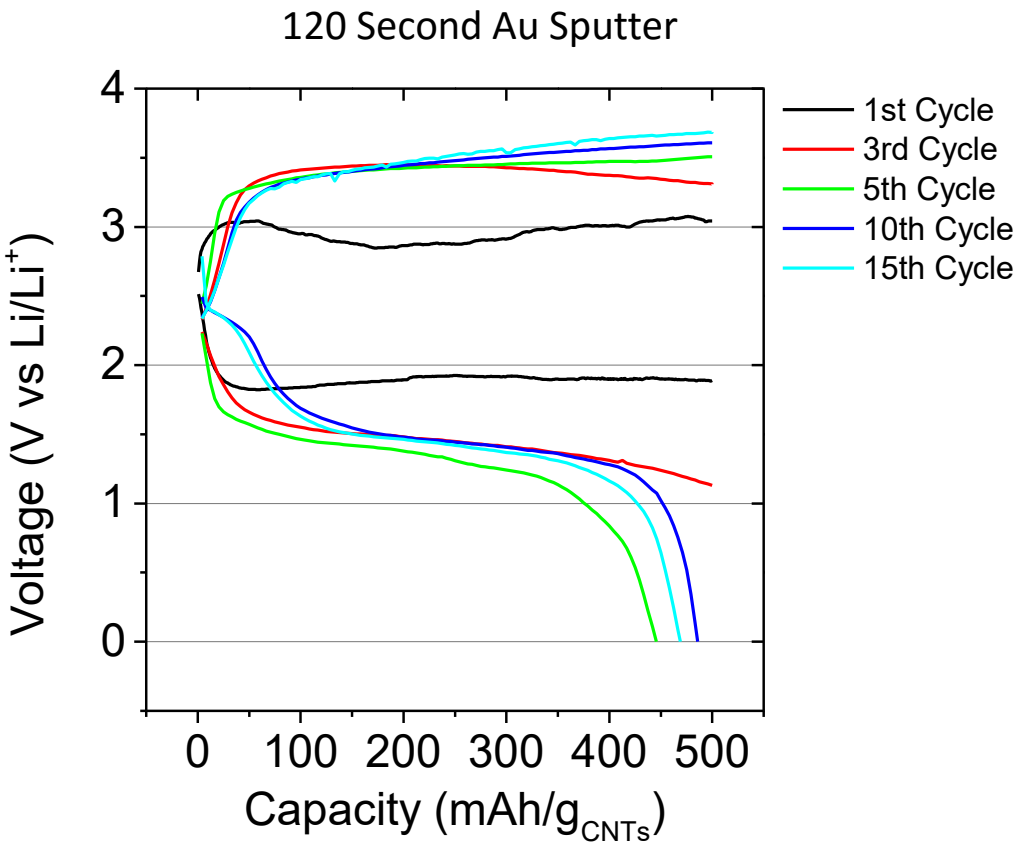

Figure 28: Charge/Discharge curve of Li-air coin cell**.** The battery architecture consisted of a lithium metal anode, 1 mg of CNTs on glass fiber cathode that was sputter coated with Au for 120 seconds, PVDF separator membrane (0.1 µm pore size), and 0.3 mL of EMIM-TFSI electrolyte. An artificial capacity limit of 500 mAh/g_{CNTs} was set with no voltage limit. The first cycle had a current density of 50 mA/g_{CNTs} and subsequent cycles were set to 250 mA/g_{CNTs}. Interestingly, the 120 second sputtered cathode had the best charging performance of the batteries studied, but experienced the worst capacity fade.

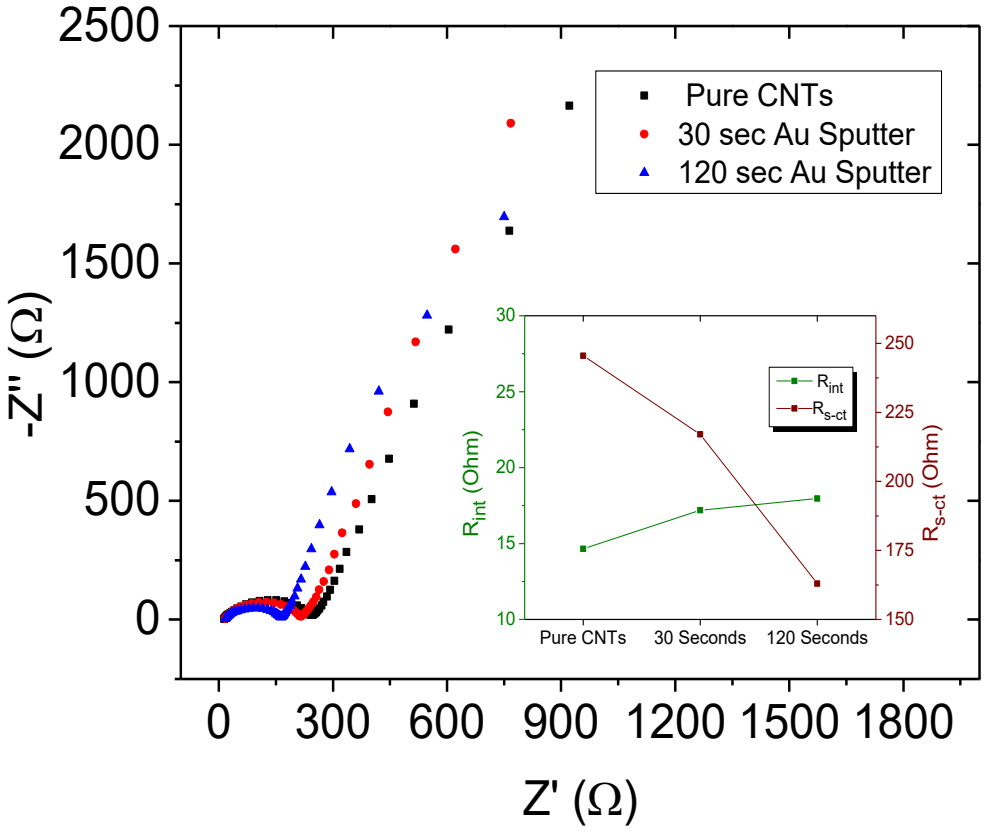

Figure 29: Impedance plot of CNTs and Au sputtered air cathodes. The inlay shows overall internal resistance R_{int} on the left-axis and a combination of the surface and charge-transfer resistances (i.e. the diameter of the semicircle of the main plot) $R_{s\text{-}ct}$ on the right-axis. The electrodes with a higher gold content show a slight increase in R_e yet show a dramatic reduction in the $R_{s\text{-}ct}$ by more than 30%.

VIII. Failure Mechanisms and System Improvement

A. Lithium foil

Upon examining the components *ex situ* after failure, we discovered that very little visible Li metal remained on the anode **[Figure 30 a]**. X-ray diffraction of the anode reveals the presence of both LiOH and Li_2CO_3, the products of Li reacting with moisture and carbon respectively **[Figure 30 b]**[*]. The ionic liquid electrolytes, despite being hydrophobic, still allows ingression of traces amounts of moisture and CO_2 among other

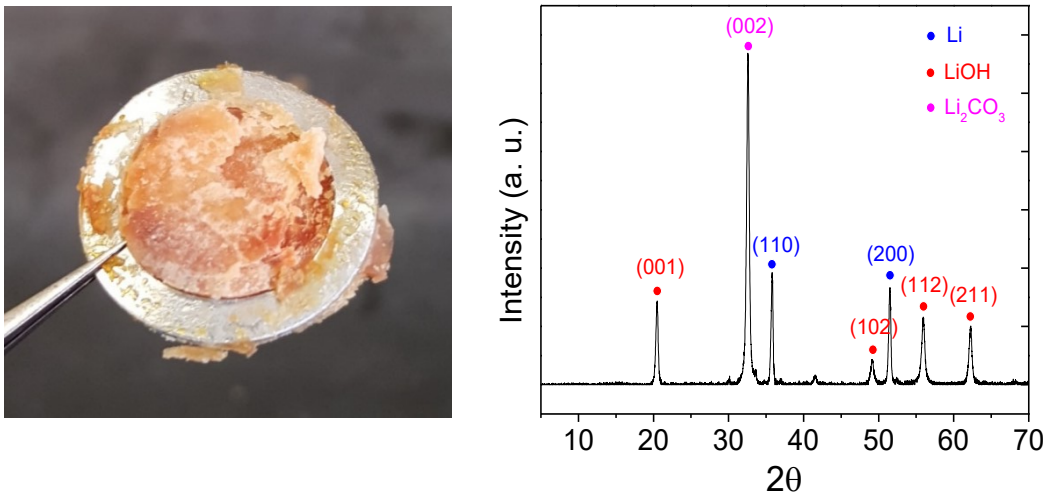

Figure 30: a) Digital photograph of a failed lithium metal anode after cycling in air cell for ~4.5 days (the silver ring is a stainless steel spring). **b)** X-ray diffraction pattern of failed anode revealing the presence of a mixture of metallic Li, LiOH and Li_2CO_3.

[*] I may add a picture of pristine Li foil

gasses[32]. These dissolved gasses cross over from the air cathode and react with the Li metal at the anode. This is likely why LiOH and Li_2 CO_3 are observed as the product at the failed anode. In order to fully test the long life performance of our air cathode we required a stable anode.

B. Lithium Titanate

Lithium Titanate (Li_2TO_3) or LTO is a anode material used in high current density batteries instead of commonly used carbon anodes. In an attempt to mitigate the stability issues that arise with a lithium metal anode, we investigated implementing lithium hosts found in Li-ion batteries into our air system. It is possible to create thin films of these materials that can be easily integrated into coin cell batteries by blade coating a slurry of the material onto metal foil. Our thin films were deposited onto 99.9% aluminum foil due to its unreactive nature to Li-air chemistry—conventional copper foil is reactive and will kill the system. The blade coating procedure can be found in the **section 3** of the supplementary information. We ran an unmodified, sealed coin cell of LTO vs Li metal as a Li-ion standard to compare to our LTO lithium-air batteries to and determine the stability of our LTO electrode **[Figure 31]**.

Figure 31: a) Charge/discharge curve of Li-air coin cell. The battery architecture consisted of a lithium metal electrode, a lithium titanate electrode, glass fiber separator membrane, and 0.3 mL of EMIM-TFSI electrolyte. No capacity limit was set, a voltage limit of 1.0 – 2.5 V was imposed. All cycles had a current density of 50 mA/g_{CNTs}. **b)** After 100 cycles the battery maintained almost 90% of charge capacity and nearly 97% of discharge capacity.

When the LTO was integrated into the Li-air coin cell it resulted in a cell that remained stable even after 50 cycles, however during discharge the polarity reversed and a negative voltage appeared **[Figure 32]**. A potential explanation for this negative voltage could arise from an undercapacity of Li available from the LTO. Our capacity limit requires 0.3 mAh of energy while 5 mg of LTO offers a theoretical 0.875 mAh of energy. It would be recommended for future studies to have a dramatic overcapacity of LTO.

Increasing current brought the battery further negative. However, LTO is known for stability in high power Li-ion batteries. Further studies are required to see if LTO can be a viable replacement for metallic lithium in our Li-air cells.

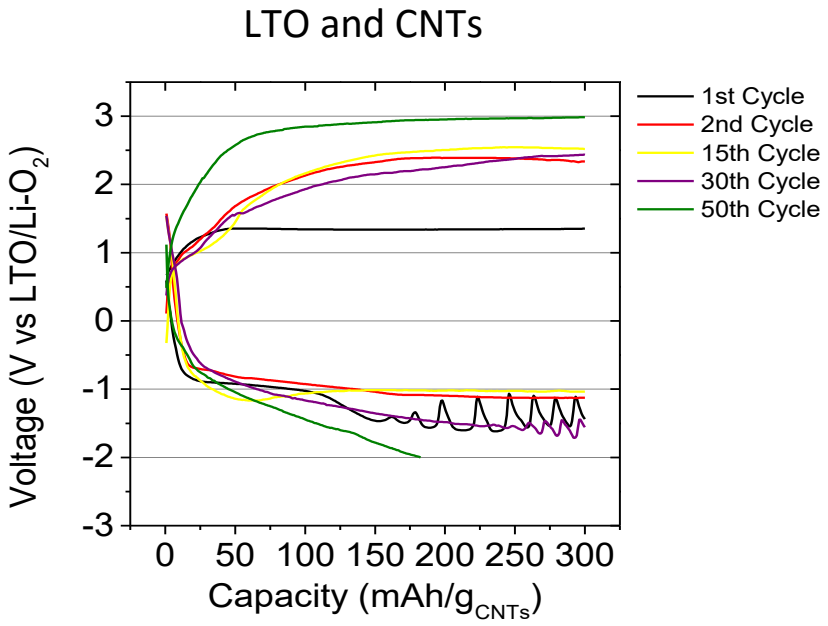

Figure 32: Charge/discharge curve of Li-ion coin cell. The battery architecture consisted of a lithium titanate anode, 1 mg of CNTs on glass fiber cathode, glass fiber separator membrane, and 0.3 mL of EMIM-TFSI electrolyte. An artificial capacity limit was set to 300 mAh/g_{CNTs} for all cycles with no voltage limit. The current density was 250 mA/g_{CNTs}.

IX. Conclusions and Future Steps

A. Results Summary

We were able to successfully develop and test working lithium-air coin cell batteries that were stable in ambient air for up to 35 cycles over the period of a week. Tests were run with high current densities of 250 mA/g_{CNTs} allowing us to charge and discharge an artificial capacity limit of 500 mAh/g_{CNTs} in only 2 hours. At lower current densities of 50 mA/g_{CNTs} were achieved a stable discharge voltages of roughly 2.6 V and charge voltage below 3.5 V for the entire set capacity. We found the addition of gold improved overall system longevity and cyclability as well as both the charge and discharge potentials. The Au also improved the surface and charge-transfer impedance of our air cathodes, however further investigation and characterization is required to fully understand the role Au plays in catalyzing the OER and ORR at the air electrode. Lithium anode stability still remains the main crux in our system.

B. Atmosphere Controllable Pressure Vessel

The instability of the lithium metal due to moisture and CO_2 crossover within the cell prompted us to build a pressure vessel to control the atmosphere that our batteries are tested in **[Figure 33]**. We are able to pressurize this vessel with any composition of gas to a wide range of pressures (rated up to 300 psi). Our next steps are to study the stability of our Li metal in an atmosphere of 20% O_2, 80% N_2 to achieve a close mimic of ambient air while eliminating moisture and CO_2 in the system. If this improves the stability of our Li metal anode, it should allow us to better focus our study on the catalytic and cyclability performance of our air cathode. Since many reactions with moisture and CO_2 also occur at the cathode, its performance should be improved as well.

Figure 33*:* Pressure vessel outfitted to test Li-air coin cell batteries.

C. Characterization Improvements

In order to perform a full investigation on the air electrode more in depth characterization is required. While electron microscopy is a powerful tool to characterize the morphology and small scale structure our battery's components, the EDAX elemental analysis system installed on the electron microscope is unable to detect Li emissions and therefore Li based products. Lithium is one of the smallest elements and consequently has a very low energy k-alpha emission line of only 0.0549 keV (compared to Au with a k-alpha of 68.8037 keV)[33]. To fully characterize and better understand the nature Li-air battery other characterization methods need to be performed. The most powerfully methods to study the products within battery systems are: mass spectroscopy, nuclear magnetic resonance (NMR), Fourier transform infrared spectroscopy (FTIR) and Raman spectroscopy[34]. Access to these tools would greatly help us to elucidate the phenomena occurring within our Li-air batteries and hopefully allow for dramatic improvements to the current technology.

[1] Key World Energy Statistics

[2] Luethi, D. et al. High-resolution carbon dioxide concentration record 650,000-800,000 years before present. Nature [London] 453, 379–382 (2008).

[3] "Emission of Greenhouse Gases in the United States 2008", U.S. Department of Energy

[4] http://www.bloomberg.com/energy

[5] IMS Research (now owned by IHS-CERA) report 'The Role of Energy Storage in the PV Industry – World – 2013 Edition'.

[6] Bruce, P. G., Freunberger, S. A., Hardwick, L. J. & Tarascon, J.-M. Li-O2 and Li-S batteries with high energy storage. *Nat Mater* **11,** 19–29 (2012).

[7] http://batteryuniversity.com/learn/article/the_high_power_lithium_ion

[8] Littauer, E. L. & Tsai, K. C. Anodic Behavior of Lithium in Aqueous Electrolytes I . Transient Passivation. *J. Electrochem. Soc.* **123,** 771–776 (1976).

[9] Abraham, K. M. & Jiang, Z. A Polymer Electrolyte-Based Rechargeable Lithium/Oxygen Battery. *J. Electrochem. Soc.* **143,** 1–5 (1996).

[10] Padbury, R. & Zhang, X. Lithium–oxygen batteries—Limiting factors that affect performance. *Journal of Power Sources* **196,** 4436–4444 (2011).

[11]Wen, Z., Shen, C. & Lu, Y. Air Electrode for the Lithium-Air Batteries: Materials and Structure Designs. *ChemPlusChem* **80,** 270–287 (2015).

[12] Jun Lu & Amine, K. Recent Research Progress on Non-aqueous Lithium-Air Batteries from Argonne National Laboratory. *Energies (19961073)* **6,** 6016–6044 (2013).

[13] Jung, H.-G., Hassoun, J., Park, J.-B., Sun, Y.-K. & Scrosati, B. An improved high-performance lithium-air battery. *Nature Chemistry* **4,** 579–585 (2012).

[14] Brandt, K. & Laman, F. C. Reproducibility and reliability of rechargeable lithium/molybdenum disulfide batteries. *Journal of Power Sources* **25,** 265–276 (1989).

[15] Tarascon, J.-M. & Armand, M. Issues and challenges facing rechargeable lithium batteries. *Nature* **414,** 359 (2001).

[16] Girishkumar, G., McCloskey, B., Luntz, A. C., Swanson, S. & Wilcke, W. Lithium−Air Battery: Promise and Challenges. J. Phys. Chem. Lett. 1, 2193–2203 (2010).

[17]Laoire, C. O., Mukerjee, S., Abraham, K. M., Plichta, E. J. & Hendrickson, M. A. Influence of Nonaqueous Solvents on the Electrochemistry of Oxygen in the Rechargeable Lithium−Air Battery. *J. Phys. Chem. C* **114,** 9178–9186 (2010).

[18] Zhang, S. S., Foster, D. & Read, J. Discharge characteristic of a non-aqueous electrolyte Li/O2 battery. *Journal of Power Sources* **195,** 1235–1240 (2010).

[19] Abraham, K. M. & Jiang, Z. A Polymer Electrolyte-Based Rechargeable Lithium/Oxygen Battery. J. Electrochem. Soc. 143, 1–5 (1996).

[20] Carvalho, D. V., Loeffler, N., Guk-Tae Kim & Passerini, S. High Temperature Stable Separator for Lithium Batteries Based on SiO2 and Hydroxypropyl Guar Gum. Membranes 5, 632–645 (2015).

[21] Lu, Y.-C.; Gasteiger, H. A.; Parent, M. C.; Chiloyan, V.; Shao-Horn, Y. *Electrochem. Solid State Lett.* **2010**, *13*, A69–A72

[22] Lu, Y.-C. *et al.* Platinum−Gold Nanoparticles: A Highly Active Bifunctional Electrocatalyst for Rechargeable Lithium−Air Batteries. *J. Am. Chem. Soc.* **132,** 12170–12171 (2010).

[23] Ogasawara, T.; Debart, A.; Holzapfel, M.; Novak, P.; Bruce, P.G. Rechargeable Li2O2 electrode for lithium batteries. *J. Am. Chem. Soc.* **2006**, *128*, 1390–1393.

[24] Lau, S. & Archer, L. A. Nucleation and Growth of Lithium Peroxide in the Li–O2 Battery. *Nano Lett.* **15,** 5995–6002 (2015).

[25] Xu, Y., Zhou, M. & Lei, Y. Nanoarchitectured Array Electrodes for Rechargeable Lithium- and Sodium-Ion Batteries. *Adv. Energy Mater.* n/a–n/a (2016). doi:10.1002/aenm.201502514

[26] Lim, H.-K. *et al.* Toward a Lithium–'Air' Battery: The Effect of CO2 on the Chemistry of a Lithium–Oxygen Cell. *J. Am. Chem. Soc.* **135,** 9733–9742 (2013).

[27] Ye, H. & Xu, J. J. Polymer Electrolytes Based on Ionic Liquids and Their Application to Solid-state Thin-film Li-Oxygen Batteries. *ECS Trans.* **3,** 73–81 (2008).

[28] Hiramatsu, H. & Osterloh, F. E. A Simple Large-Scale Synthesis of Nearly Monodisperse Gold and Silver Nanoparticles with Adjustable Sizes and with Exchangeable Surfactants. *Chem. Mater.* **16,** 2509–2511 (2004).

[29] Kang, Y., Ye, X. & Murray, C. B. Size- and Shape-Selective Synthesis of Metal Nanocrystals and Nanowires Using CO as a Reducing Agent. *Angewandte Chemie International Edition* **49,** 6156–6159 (2010).

[30] Barisci, J. N., Wallace, G. G., MacFarlane, D. R. & Baughman, R. H. Investigation of ionic liquids as electrolytes for carbon nanotube electrodes. *Electrochemistry Communications* **6,** 22–27 (2004).

[31] Kuboki, T., Okuyama, T., Ohsaki, T. & Takami, N. Lithium-air batteries using hydrophobic room temperature ionic liquid electrolyte. *Journal of Power Sources* **146,** 766–769 (2005).

[32] Althuluth, M., Mota-Martinez, M. T., Kroon, M. C. & Peters, C. J. Solubility of Carbon Dioxide in the Ionic Liquid 1-Ethyl-3-methylimidazolium Tris(pentafluoroethyl)trifluorophosphate. *J. Chem. Eng. Data* **57,** 3422–3425 (2012).

[33] J. A. Bearden*, "X-Ray Wavelengths*", *Review of Modern Physics, (January 1967) pp. 86-99*

[34] Peter Bruce. *The Lithium Air Battery: Fundimentals*.

Supplementary Information

1. Characterization Instruments

a. TEM:

All Transmission electron microscopy imaging was performed on a 120 kV, FEI Tecnai 12 TWIN microscope

b. SEM:

All scanning electron microscopy imaging was performed with a JEOL JSM-6700F Field Emission Scanning Electron Microscope

c. EDAX:

Compositional analysis was performed using an EDAX Apollo XL detector and Genesis 4000 software with Bulk Method quantification using ZAF algorithm

d. XRD:

X-ray diffraction (XRD) patterns were collected on a PANalytical X'Pert^3 Powder X-Ray Diffractometer equipped with a Cu Kα radiation source (λ=0.15406)

e. Battery Tester:

Arbin BT 2000 linear battery testing system

f. Impedance Tester:

Autolab PGSTAT302N potentiostat/galvanostat

Intended to be blank

2. Nanoparticle and Nanowire Dispersion

a. Hexanes

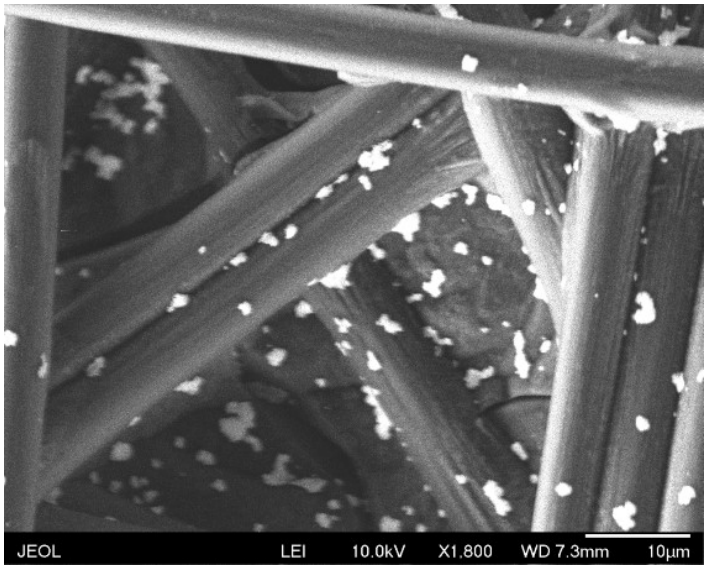

b. Toluene

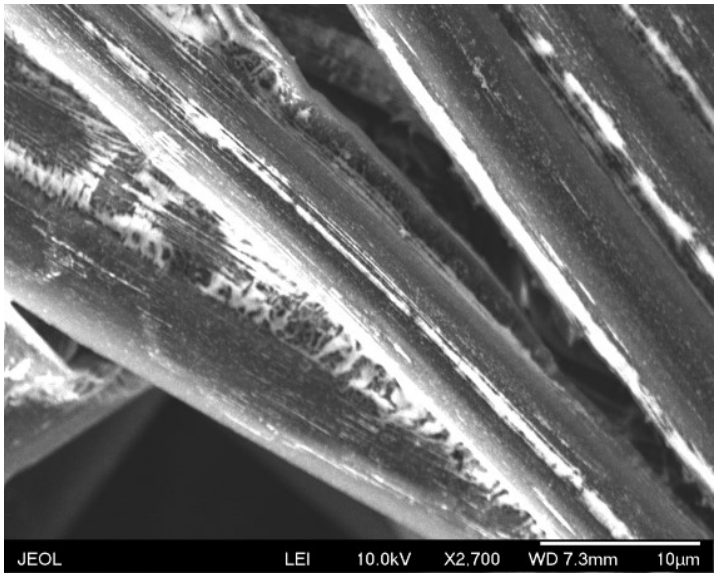

c. Sonicated Wires

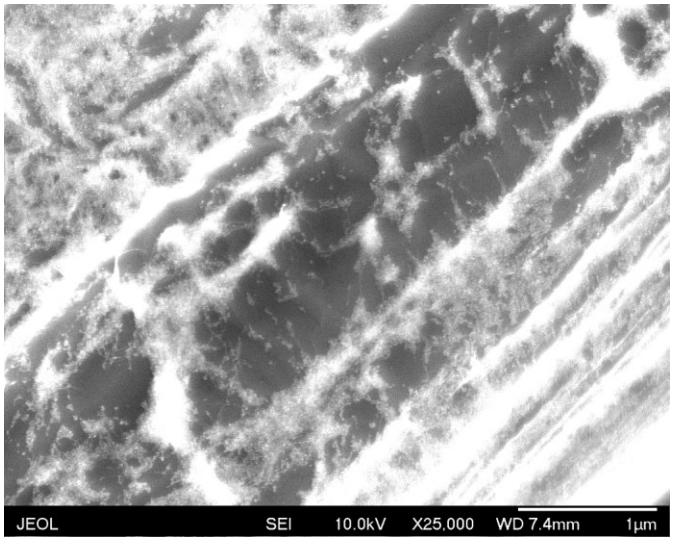

3. Lithium Host Slurry and Blade Coating Methods

LTO, carbon black, and PVDF binder in a 4:4:1 ratio was mixed in NMP solvent for 2 days to insure homogeneity. This was the coated onto aluminium foil using a doctors blade with a height of 200 µm. the foil was placed in an oven overnight at 80° C to evaporate off the solvent. The foil was pressed between two rolled with a gap space of 20 µm to improve adhesion to the Al foil. The foil was then cut into 15 mm disks and are ready to use in the battery.

4. LTO Lithium-air Testing

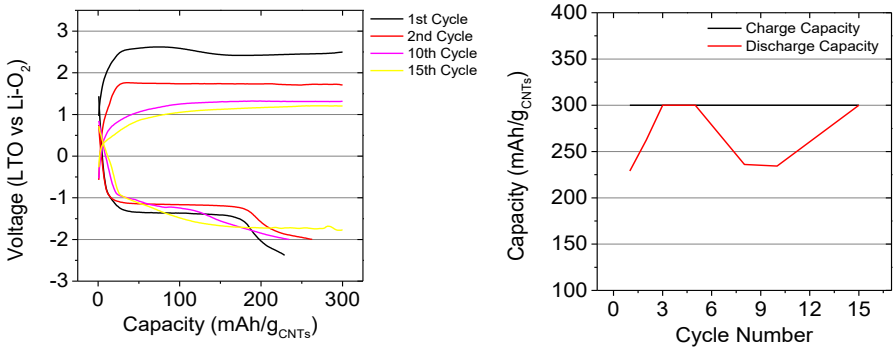

Pure CNTs vs LTO. 300 Cap limit. -2.0 V limit.

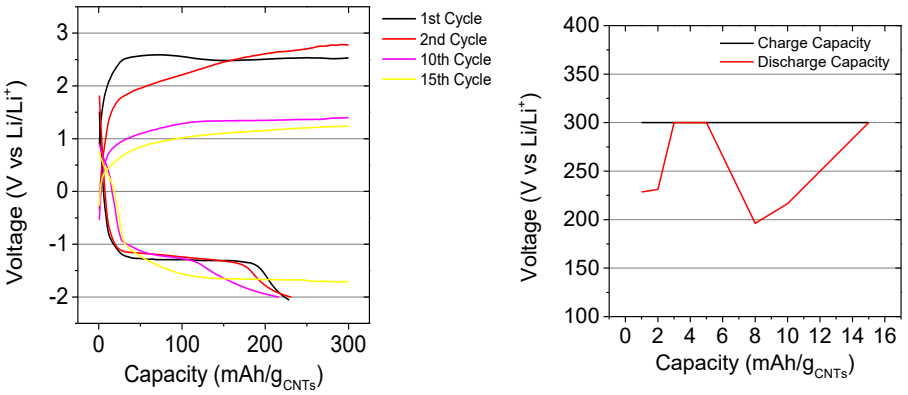

CNTs with 30 sec Au sputter vs LTO. 300 Cap limit. -2.0 V limit.

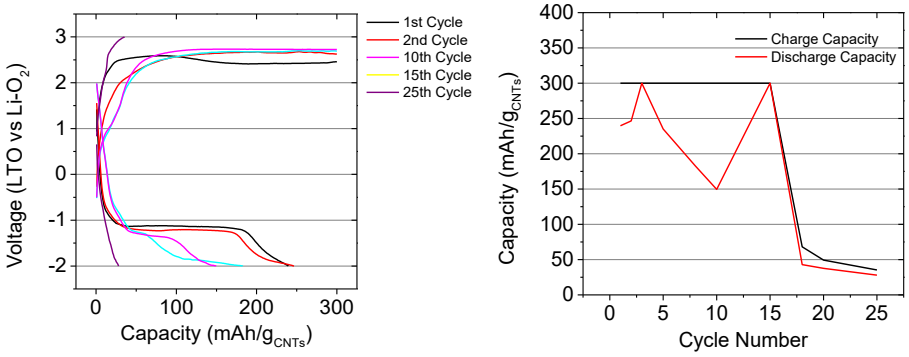

CNTs with 120 sec Au sputter vs LTO. 300 Cap limit. -2.0 V limit.

5. Size Control of Au Nanoparticles

a. 20 nm

The same method was used as describe in the body of the thesis, however to produce gold nanoparticles 20 nm in size only 36 mg of $HAuCl_4$ was used instead of 54 mg. 0.5 mL of oleic acid can be added to improve the monodispersity of the nanoparticles, but it is not a necessary component.

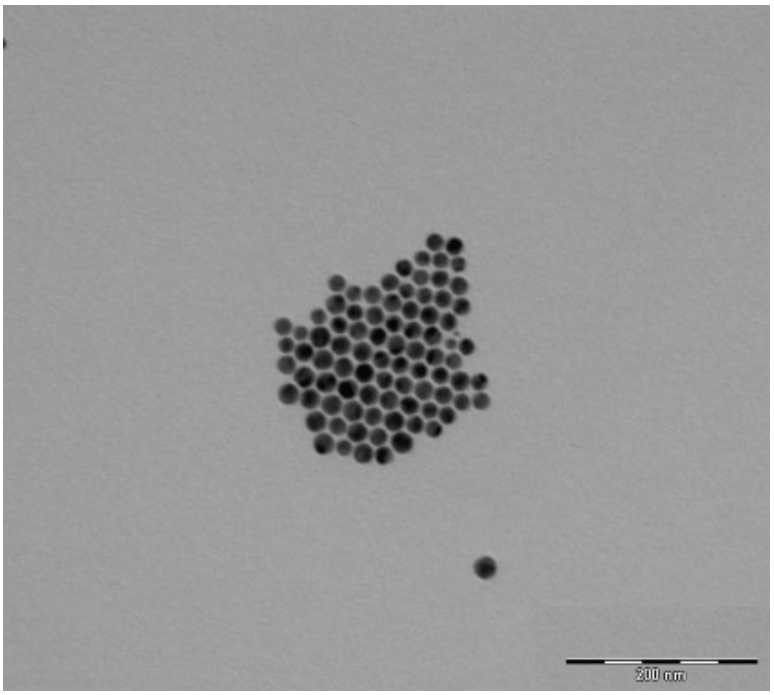

6. Thick Nanowires

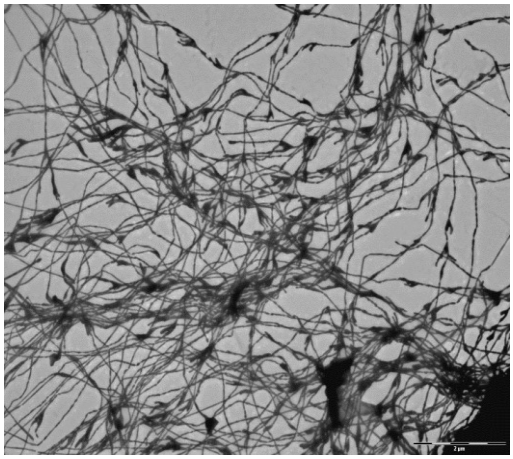

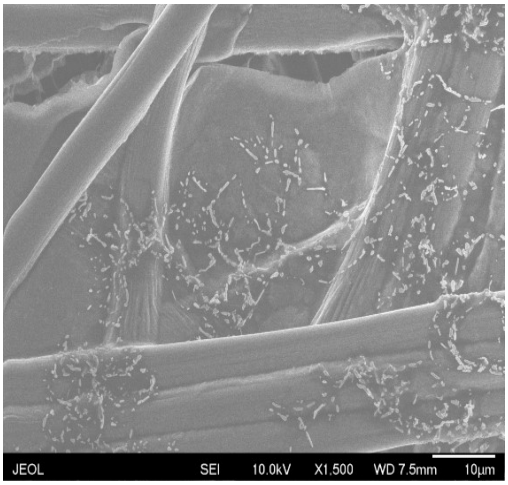

Attempts to synthesis thicker gold nanowires. Method modified from Zhu, C. *et al.* Facile Synthesis of Gold Wavy Nanowires and Investigation of Their Growth Mechanism. *J. Am. Chem. Soc.* **134,** 20234–20237 (2012). Transmission electron microscopy of sea kelp-like gold nanowires. Scale bars represent 2 µ and 10 µ respectively. Scanning electron micrograph of wires on carbon paper anneal at 120° C overnight. These wires also broke apart into smaller

Intended to be blank

EDUCATION

The Johns Hopkins University
BALTIMORE, MD
M.S. Chemical and Biomolecular Engineering *Expected Graduation: May 2016*
Graduate GPA: 3.61
B.S. Materials Science Engineering, *Concentration: Nanotechnology* *May 2015*
Minor: Entrepreneurship and Management
Undergraduate GPA: 3.05 | Dean's List: Spring 2014, Spring 2015

Relevant Courses
Interfacial Sciences with Applications to Nanoscale Systems, Advanced Thermodynamics and Kinetics, Advanced Transport Phenomena, Nanomaterials Senior Design I & I, Electronics and Instrumentation, Materials Science of Energy Technologies, Nanomaterials Lab, Micro and Nano Structured Materials and Devices, Differential Equations, Linear Algebra, Calculus I, II & III, Engineering Business and Management, Leadership in Teams, Principles of Managements

RESEARCH & EXPERIENCE

Dr. Chao Wang Group, JHU Chemical and Bimolecular Engineering BALTIMORE, MD
Research Assistant
Jan 2013-Present

- Led project in studying noble metal nanoparticles for use as oxygen reduction (ORR) and oxygen evolution reaction (OER) catalysts in Zinc and Lithium-Oxygen batteries
- Developed nanoparticle synthesis techniques and thin film technologies for electrode materials in Zinc-air and Lithium-ion batteries
- Developed nanoparticle synthesis techniques for applications in catalytic CO_2 capture, oxygen reduction and oxygen evolution reactions

Visiting Scholar and Intern at IMEC under Dr. Philippe Vereecken LEUVEN, BELGIUM
Research Assistant [IMEC Laboratories] Large Area Electronics Division *May-July 2014*

- Selected as one of four Johns Hopkins students to spend a summer performing research in Leuven Belgium through the JHU Institute of Nano and Bio Technology
- Initiated a project to synthesize and implement $LiMnO_2$ nanoparticles for applications in thin film Li-ion batteries
- Presented findings to a group of IMEC principal investigators, post doctorates, KU Leuven PhD students and members of Johns Hopkins Institute of Nano and Biotechnology with continuing collaboration between JHU and IMEC

Baxter Health Care WESTLAKE
VILLAGE, CA *Intern-BioScience & Global Marketing Divisions*
June-July 2010

- Researched and developed a strategy to help optimize the marketing efforts of Baxter's surgical devices in a global environment
- Presented findings to the principals of BioScience and BioScience Global Marketing divisions
- Arranged for advertisement space in over 10 surgical journals, both physical and electronic formats

TECHNICAL & SUPPORTING SKILLS

- Advanced chemical synthesis, electrochemical and materials laboratory experience including use of potentiostat and other electrochemical tools, Transmission Electron Microscopy, X-Ray Diffraction, Scanning Electron Microscopy and glove box
- Self-starter: able to initiate and conduct research as evident by lithium-oxygen research, PURA and IMEC work
- Proficient in Autolab, NOVA, Origin, Comsol Multiphysics, MatLab, Mathmatica, basic Java and Microsoft Suite
- Naturally inquisitive, versatile, good management and leadership skills, adaptable and quick to learn and self-teach

PUBLICATIONS & AWARDS

Publication Accepted:
BALTIMORE, MD
Published in The Journal of Nano Energy *September 2015*
David Raciti; Joseph Kubal; Cheng Ma; Michael Barclay; **Matthew Gonzalez**; Miaofang Chi; Jeffrey Greeley; Karren L. More; Chao Wang, PhD. "Pt_3Re Alloy Nanoparticles as Electrocatalysts for the Oxygen Reduction Reaction." 10.1016/j.nanoen.2015.12.014

Vredenburg Scholarship
BALTIMORE, MD
Recipient
March 2014

- Awarded an $8,000 scholarship by Johns Hopkins Whiting School of Engineering to travel and participate in international research at the Technischen Universität Berlin under Dr. Peter Strasser

Provost's Undergraduate Research Award (PURA)
BALTIMORE, MD
Recipient
May 2013

- Awarded $2500 grant from The Johns Hopkins University for morphologically controlled Cu-Ni alloy nanoparticle synthesis research
- Spent sophomore summer at JHU developing novel organometallic nanoparticle synthesis techniques

LEADERSHIP & EXTRACURRICULARS

Teaching Assistant
BALTIMORE, MD
Leadership and Management in Material Science and Engineering *Fall 2015*

- Assisted with teaching leadership and management skills to a class of 20 senior engineering majors
- Graded and provided feedback on assignments taught from Harvard Business School case studies

Materials Science Undergraduate Lab
Spring 2015

- Assisted with experiments, hands-on teaching and grading lab reports

Johns Hopkins - Men's Varsity Water Polo
BALTIMORE, MD
Division III Eastern Champions
January 2011 & 2012
NCAA Division III National Champions
January 2012

Phi Kappa Psi Fraternity
BALTIMORE, MD
Recruitment Chair *January 2013*

- Helped create and manage a budget of $5,000 for the two week fraternity recruitment process

Standards Board *September 2013-2015*

- Responsible for upholding and enforcing the financial, social and ethical obligations required by the national fraternity

SABES (STEM Achievement in Baltimore Elementary Schools) BALTIMORE, MD
Mentor *August 2013-Present*

- Aid with teaching an afterschool program to improve educational outcomes in STEM disciplines throughout Baltimore City's elementary schools

Materials Research Society-JHU
BALTIMORE, MD
Member *2012-2105*

- Met monthly to discuss current material science developments
- Attended weekly seminar talks given by guest speakers on current and developing materials technologies